Available online at www.sciencedirect.com

SCIENCE DIRECT®

International Journal of Coal Geology 66 (2006) 69–107

International Journal of COAL GEOLOGY

www.elsevier.com/locate/ijcoalgeo

Stratigraphic distribution of macerals and biomarkers in the Donets Basin: Implications for paleoecology, paleoclimatology and eustacy

A. Izart [a,*], R.F. Sachsenhofer [b,*], V.A. Privalov [c], M. Elie [a], E.A. Panova [d], V.A. Antsiferov [c], D. Alsaab [a], T. Rainer [b], A. Sotirov [b], A. Zdravkov [b], M.V. Zhykalyak [e]

[a] *UMR 7566G2R, Université Henri Poincaré, BP239, F-54506, Vandoeuvre-les-Nancy, France*
[b] *Institut für Geowissenschaften, Montanuniversität Leoben, A-8700 Leoben, Austria*
[c] *Donetsk National Technical University, Artem str. 58, UA-83000 Donetsk, Ukraine*
[d] *UkrNIMI, National Academy of Science of Ukraine, Tchelyuskintsev str. 291, UA-83121 Donetsk, Ukraine*
[e] *Donetsk State Regional Geological Survey, Sybirtseva str. 17, UA-84500 Artemovsk, Ukraine*

Received 3 May 2005; received in revised form 27 June 2005; accepted 11 July 2005
Available online 22 September 2005

Abstract

More than one hundred and thirty coal seams and coaly layers occur in the Donets Basin (Donbas). Twenty-eight (52 samples) of them, ranging in age from Serpukhovian (Late Mississipian) to Gzhelian (Late Pennsylvanian), 33 clastics and three limestones were studied in terms of maceral composition, sulphur contents, and biomarker distribution. Diterpanes are used to estimate the contribution of different groups of plants and the height of the water table in the swamp; hopanes are a measure of bacterial activity in the peat; and steranes indicate the relative input of wood and algae. Stratigraphic trends in these parameters are discussed in relation to paleoenvironment, climatic changes, and eustacy. A tropical climate prevailed in the Donbas from Serpukhovian to Kasimovian times. Nevertheless, periods with drier and wetter conditions can be distinguished based on maceral and biomarker data. Relatively dry conditions are observed during Serpukhovian and Vereian times, whereas wetter climates with a maximum of coal deposition occurred during the (late) Bashkirian, most of the Moscovian, and the earliest Kasimovian. No economic coal seams are hosted in upper Kasimovian and Gzhelian deposits, a result of a change to an arid climate. Our data also suggest climatic changes during sequences of different order. For the second-order, third-order, and fourth-order sequences, relatively dry or wet conditions occurred during coal deposition in the lowstand systems tract, an intermediate climate during the transgressive systems tract and the maximum flooding, and a wet climate during the highstand systems tract. The results for high frequency sequences support the Cecil's paleoclimatic model: an intermediate paleoclimate during LST (sandstone and levee siltstone), a wet climate during early TST (coal), and a dry climate during late TST (limestone), MFS (claystone), and HST (deltaic siltstone). Coals deposited

* Corresponding authors.
E-mail address: izart.alain@wanadoo.fr (A. Izart).

0166-5162/$ - see front matter
doi:10.1016/j.coal.2005.07.002

during maximum flooding periods are more enriched in C_{27} steranes derived from algae, and contain lower proportions of C_{29} steranes derived from the wood of higher plants.

Keywords: Ukraine; Carboniferous; Organic geochemistry; Molecular geochemistry; Coal petrography

1. Introduction

The Donets Basin (Donbas), located mainly in the Ukraine with the eastern part of the basin extending into Russia, contains one of the major coal fields in the world. The basin covers an area of 60,000 km^2 and is located between the Dniepr–Donets Basin and the buried Karpinsky Swell (Fig. 1).

The Carboniferous succession in the Donbas hosts about one 130 seams, each with a thickness of over 0.45 m. Coal rank is generally high and reaches the meta-anthracite stage. Low-rank coals are restricted to the western and northern basin margins (Fig. 1; Sachsenhofer et al., 2002). Main aim of a former paper (Sachsenhofer et al., 2003) was to reconstruct the depositional environment of nine seams.

In the present paper, 28 coal seams, 33 clastic rocks and three limestones are studied using a multidisciplinary approach involving organic petrographical and geochemical techniques. The seams range from Serpukhovian (Late Mississippian) to Gzhelian (Late Pennsylvanian) in age and include the economically most important coals. Main aim of this paper is to describe stratigraphic variations of maceral composition, sulphur content, and biomarker distributions in Donbas coal seams and associated rocks, and to discuss them in relation to changes in paleoenvironment, paleoclimate and eustacy. Our data from Donbas will be compared with samples from other paralic and limnic coal basins of western Europe and the paleoclimatic model of Cecil et al. (2003) that described the mid-Pennsylvanian climate across North America.

2. Geological setting and sequences

The Donets Basin forms part of the Pripyat–Dniepr–Donets–Karpinsky Basin (Fig. 1), which is a late Devonian rift structure located on the southern part of the Eastern European craton (Stovba and Stephenson, 1999; Stephenson et al., 2001). Some important aspects of the evolution of the basin are summarized in Fig. 2. Total thickness of Devonian pre- and syn-rift rocks is 750 m at the margins of the Donets Basin, but reaches 6 km along the basin center (Maystrenko et al., 2003).

Major post-rift subsidence occurred during the Permo-Carboniferous. The Carboniferous sequence, up to 14-km thick, is subdivided into lithostratigraphic units named suites A (C_1^1), B (C_1^2), C (C_1^3), to P (C_3^3) (Lutugin and Stepanov, 1913). Their correlation with the standard time-scale is presented in Fig. 2. A sequence stratigraphic frame for the Permo-Carboniferous rocks was provided by Izart et al. (1996, 1998, 2003). The coal-bearing sequence is composed of fluvial sandstone, coal, marine claystone or limestone, and deltaic claystone and siltstone. Sequences of different order can be distinguished in the Donbas: high frequency (HFS, fifth and fourth order, < 200 ka), fourth order (FOS, 100 ka to 1 Ma), third order (TOS, 1 to 5 Ma), and second order (SOS, 5 to 10 Ma). The durations of sequences are average durations obtained by division of duration of stages by number of sequences and also calculated durations by spectral analysis (Izart et al., 2003). The radiochronologic data charts of Hess and Lippolt (1986) and Menning et al. (1997) were chosen for the Carboniferous. A HFS is equivalent to a parasequence of the sequence stratigraphy (Van Wagoner et al., 1988), FOS consist of several HFS, TOS of several FOS, and SOS of several TOS.

3. Samples and methods

The samples represent 28 Serpukhovian to Gzhelian coal seams including seven Moscovian and two Serpukhovian seams studied by Sachsenhofer et al. (2003). Most Moscovian seams are represented by 5 to 11 samples (see Sachsenhofer et al., 2003 for

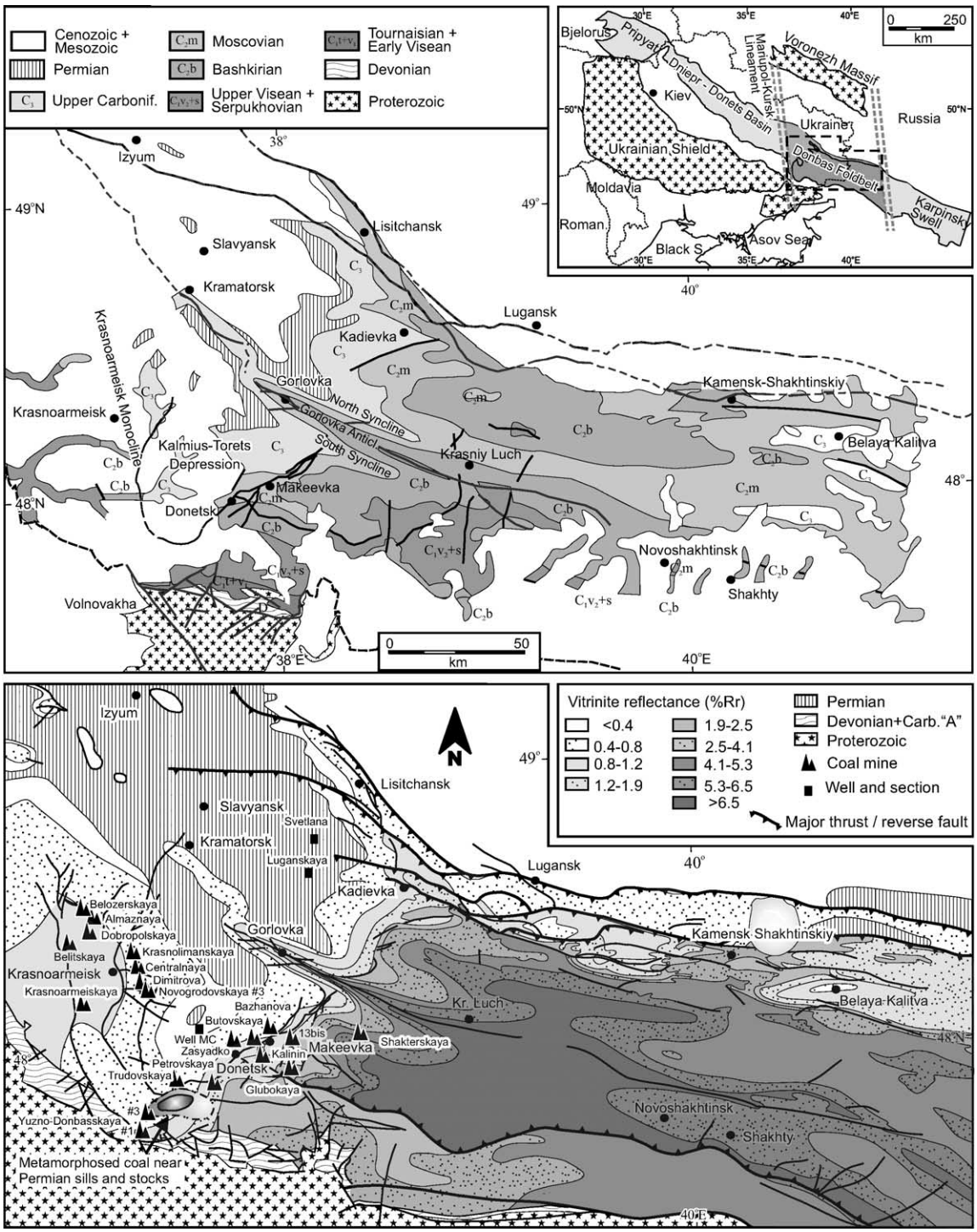

Fig. 1. Geological sketch map of the Donets Basin (modified after Popov, 1963), and coalification map at the top of the Carboniferous sequence (modified after Levenshtein et al., 1991). The position of the studied coal mines, wells and sections is shown in the vitrinite reflectance map.

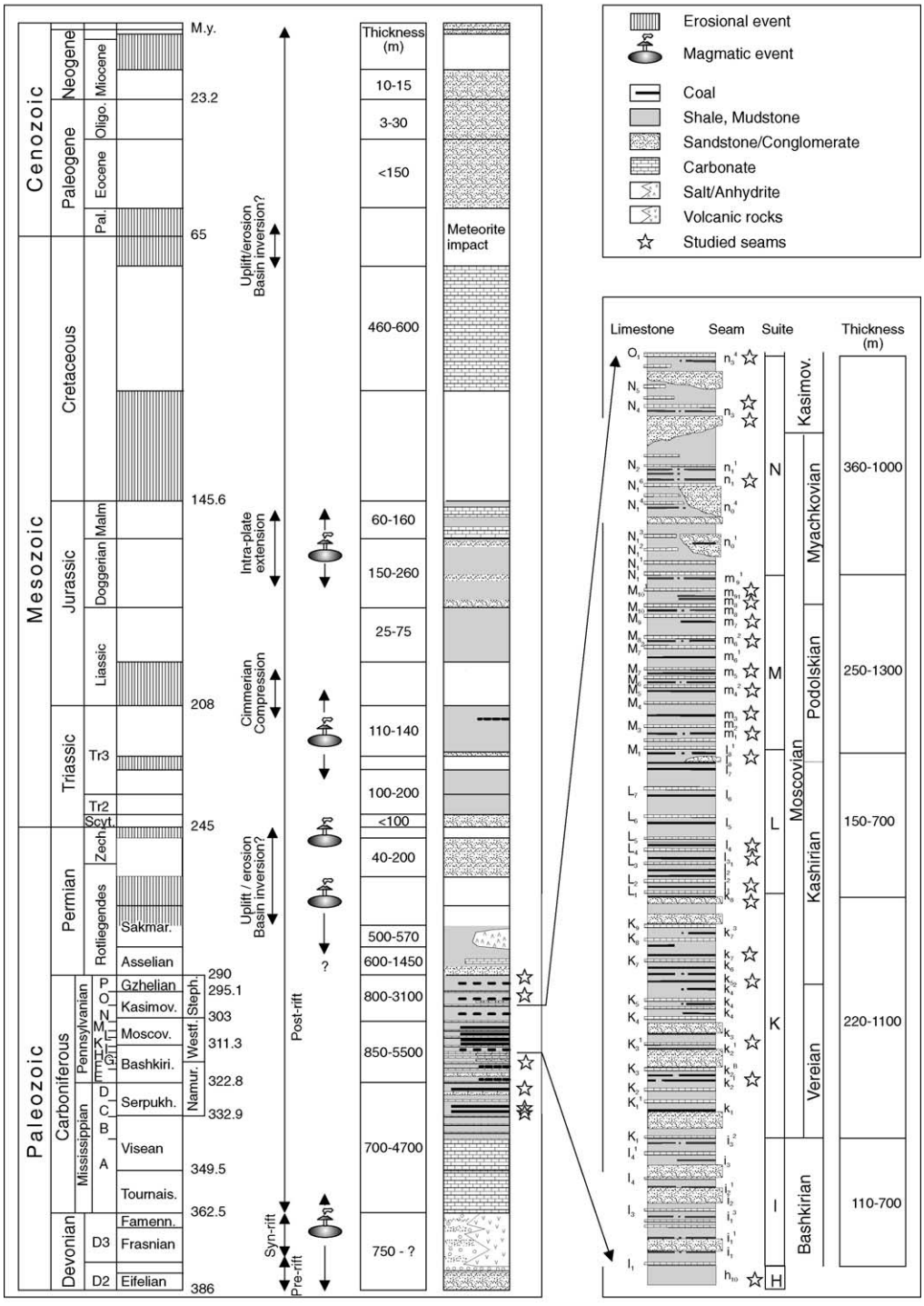

Fig. 2. Chrono- and lithostratigraphy of the Donets Basin. Major magmatic and tectonic events are shown (Sterlin et al., 1963; Belokon, 1971; Einor, 1996; Privalov et al., 1998; Stovba and Stephenson, 1999). A detailed stratigraphic column is provided for the Moscovian sequence.

detailed seam sections). Apart from these, each seam is represented by one to four samples. The sample code in Table 1 (e.g. $1n_1$ But) contains a number (1, only in cases where several samples have been taken along vertical seam sections), the name of the coal seam (n_1), and the name of the coal mine (But for Butovskaya; see Fig. 1 for mine locations). Thirty-three Podolskian to lower Kasimovian clastic rocks and three limestones from boreholes MC 598 and MC 599 (Fig. 3) were included in the study to assess changes related to lithology and within high frequency sequences. Their results are listed in Table 3 with indication of the nearest limestone bed and coal seam.

For petrographical investigations, a representative part of each of the 120 coal samples was mounted in epoxy resin, ground, and polished. Vitrinite reflectance (VR% R_r) was measured according to established procedures (Taylor et al., 1998; Table 1). At least 300 points were counted on a Leitz microscope using reflected white and fluorescent light to provide data for maceral analyses. For each sample the relative amounts of maceral groups (Table 1) were calculated. The maceral abundances refer to percentages on a mineral matter free basis (vol.% mmf). To expand our data base in terms of stratigraphic coverage, maceral data of low-rank coals (<1% R_r) provided by the Donetsk State Regional Geological Survey were also used.

For chemical analysis (Table 1), a representative portion of the sample was crushed to <250 μm to determine sulphur and total organic carbon (TOC) contents on a Leco CS-300 instrument. Ash yield and moisture content analyses followed standard procedures (Deutsches Institut für Normung, 1978, 1980). All ash yields and sulphur contents are given as weight percents on a dry basis (db). Rock Eval pyrolysis (Table 1) was performed in duplicate using a Rock Eval 2+ instrument (Espitalié et al., 1977, Peters, 1986). The amount of hydrocarbons released from kerogen during gradual heating in a helium stream was normalized to TOC to give the hydrogen index (HI) defined as S2/TOC (Espitalié et al., 1977). The bitumen index (BI), defined as S1/TOC (Killops et al., 1998), and the quality index (QI), defined as (S1+S2)/TOC (Pepper and Corvi, 1995), were also calculated. As a maturation parameter, the temperature of maximum hydrocarbon generation (T_{max}, °C) was determined. To characterize the molecular fraction, the powdered whole sediments were extracted by chloroform at 60 °C for 45 min. The total extract obtained was fractionated by liquid chromatography on a silica column into saturates, aromatics and polars. Saturates and aromatics were analysed by gas chromatography–mass spectrometry in the laboratory of the UMR G2R. The gas chromatograph was a Hewlett–Packard 5890 Series II and the detector a HP 5971 mass-selective detector, operating in "fullscan" or "single ion" (SIM) modes. The area of each peak of biomarker was measured on SIM chromatograms and ratio of various biomarkers calculated. Reference standards were not employed. Fifty-two samples of coal, two fluviatile sandstones, four levee siltstones, three marine limestones, four lacustrine claystones, 11 marine claystones and 12 deltaic siltstones were analysed by gas chromatography (Tables 2 and 3). A part of these analyses was already published (Sachsenhofer et al., 2003, Fig. 14 and Table 4) and Privalov et al. (2003a,b).

Geochemical and petrographical parameters are known to be affected by maturity. Therefore, the study concentrates on low-rank coals (<0.9% R_r) and only eight samples have a VR >0.9% R_r. Moreover, the relationships between maceral percentages, extraction yields, abundance and ratios of biomarkers, and VR are studied in a first part of the paper to assess whether any of the observed stratigraphic trends are related to changes in maturity.

4. Results

4.1. Macerals

Donbas coals are generally rich in vitrinite, with average contents of 81% (Fig. 4, Tables 1 and 5). Inertinite and liptinite macerals have mean contents of 12% and 7%, respectively. Some Serpukhovian and Vereian samples exhibit higher inertinite (58%) and liptinite (26%) percentages.

Liptinite is not visible in high-rank coals (>1.4% R_r, Fig. 5a). The same value of VR for the liptinite end was noted by Alpern and Lemos de Sousa (2002, their Fig. 27). Therefore, there is a negative correlation between liptinite percentages and VR. The low correlation coefficient ($R^2=0.33$) reflects the highly variable liptinite contents in low-rank coals.

Table 1
Petrographic, chemical and Rock–Eval data of Donbas coals

Samples	Coal mines	Vitr.	Inert.	Lipt.	Min.Mat.	Vitr.Refl.	Ash	Sulphur	TOC	Tmax	BI	HI	QI	FOS	TOS	SOS	AGE
		vol.% (mmf)			vol.%	% R_r		(% db)		(°C)	mgHC/gTOC						
p_5 Lug	Luganskaya section						58.9	3.1	27.6	433	1.7	325	326.7	HST	LST	HST	Gzhelian
o_2 Svet	Svetlana quarry	88	7	5	3	0.48	11.3	1.2	52.0	441	1.7	55	56.7	HST	HST	HST	Kasimovian
n_3^6 MC 599	MC 599 borehole	73	4	23	1	0.63	5.0	3.6	74.5	431	7.1	243	250.1	TST	TST	TST	Kasimovian
n_2^3 MC 599	MC 599 borehole	78	16	6	7	0.65	21.1	9.3	60.2	431	7.8	231	239.2	HST	LST	LST	Kasimovian
n_2^2 MC 599	MC 599 borehole	65	29	6	19	0.7		13.2	53.0	432	11.6	258	269.6	HST	LST	LST	Kasimovian
$5n_1$ But	Butovskaya Donetskaya	72	15	13	2	0.63	4.3	2.9	77.4	436	12.5	306	318.5	MFS	HST	HST	Myachkovian
$4n_1$ But	Butovskaya Donetskaya	56	32	12	1	0.75	11.6	1.5	75.5	438	8.7	244	252.7	MFS	HST	HST	Myachkovian
$3n_1$ But	Butovskaya Donetskaya	73	16	11	1	0.79	2.0	1.2	82.0	444	7.9	262	271.9	MFS	HST	HST	Myachkovian
$2n_1$ But	Butovskaya Donetskaya	82	12	6	1	0.83	6.9	1.4	77.9	442	8.1	255	263.1	MFS	HST	HST	Myachkovian
$1n_1$ But	Butovskaya Donetskaya	82	10	8	2	0.84	9.5	1.7	75.7	437	8.3	254	262.3	MFS	HST	HST	Myachkovian
n_1 But Mak	Butovskaya Makeevka					1.7				535				MFS	HST	HST	Myachkovian
$2m_9$ MC 598	MC 598 borehole	77	15	8	9	0.80		8.5	61.8	447	19.3	193	212.5	LST	LST	HST	Myachkovian
$1m_9$ MC 598	MC 598 borehole	82	10	8	3	0.78		4.4	66.0	448	20.2	200	219.9	LST	LST	HST	Myachkovian
m_8^1 Sch 1355	Sch 1355 borehole	80	12	8	5	0.83	10.9	2.8						LST	LST	HST	Podolskian
m_7 MC 598	MC 598 borehole	88	7	5	7	0.79		6.7	69.4	448	20.7	190.7	211.4	TST	HST	HST	Podolskian
m_6^3 Sch 1355	Sch 1355 borehole	82	13	5	18	0.76	31.6	3.8						HST	HST	HST	Podolskian
$2m_5$ Alm	Almaznaya	79	14	7	1	0.73	1.3	1.3	79.9	435	2.4	246	248.4	TST	MFS	MFS	Podolskian
$4m_4$ Dob	Dobropolskaya	81	11	8	0	0.7	4.2	2.1	78.1	438	3.9	204	207.9	HST	MFS	MFS	Podolskian
m_3 Trudo	Trudovskaya	90	4	6	0	0.39	2.9	2.3	68.7	418	1.6	219	220.6	TST	TST	MFS	Podolskian
m_3 Za	Zasyadko	72	25	3	1	0.82	3.4	1.6	84.5	449	13.7	179	192.7	TST	TST	MFS	Podolskian
$1m_2$ Bel	Belozerskaya	87	6	7	15	0.71	21.2	8.0	61.7	433	6.3	290	296.3	MFS	TST	MFS	Podolskian
$1l_8$ Bel	Belozerskaya	92	5	3	3	0.79	4.7	1.0	75.7	444	3.6	228	231.6	HST	HST	MFS	Podolskian
l_4 Trudo	Trudovskaya	83	10	7	0	0.52	0.8	0.9	75.9	431	3.7	165	168.7	HST	HST	TST	Kashirian
$8l_3$ Alm	Almaznaya	89	6	5	0	0.91	1.8	1.3	83.6	449	3.1	200	203.1	MFS	MFS	TST	Kashirian
$1l_3$ Bel	Belozerskaya	86	6	8	3	0.87	3.4	3.1	81.9	445	10.6	217	227.6	MFS	MFS	TST	Kashirian
$3l_1$ Nov	Novogrodovskaya	85	3	12	1	0.71	2.9	4.0	77.7	437	9.6	244	253.6	MFS	MFS	TST	Kashirian

$1l_1$ Dob	Dobropolskaya	88	8	4	4	0.78	13.2	2.5	51.9	432	7.5	276	283.5	HST	MFS	TST	Kashirian
$9l_1$ Dim	Dimitrova	67	24	9	5	0.71	9.3	5.7	73.1	442	10.1	245	255.1	HST	MFS	TST	Kashirian
$8l_1$ Dim	Dimitrova	70	22	8	5	0.72	10.0	3.3	77.1	443	11.1	224	235.1	HST	MFS	TST	Kashirian
$6l_1$ Dim	Dimitrova	78	15	7	0	0.74	2.3	3.6	81.1	442	18.1	242	260.1	HST	MFS	TST	Kashirian
$5l_1$ Dim	Dimitrova	71	18	11	1	0.73	1.5	3.4	83.8	442	11.4	248	259.4	HST	MFS	TST	Kashirian
$4l_1$ Dim	Dimitrova	72	18	10	6	0.76	13.6	2.9	71.0	441	9.3	250	259.3	HST	MFS	TST	Kashirian
$3l_1$ Dim	Dimitrova	83	6	11	1	0.77	4.1	5.5	80.1	439	14.7	263	277.7	HST	MFS	TST	Kashirian
$2l_1$ Dim	Dimitrova	81	8	11	2	0.76	3.3	3.5	81.9	440	14	253	267	HST	MFS	TST	Kashirian
$1l_1$ Dim	Dimitrova	80	15	5	10	0.74	8.3	7.4	75.3	438	11.4	248	259.4	HST	MFS	TST	Kashirian
$1k_8$ Dob	Dobropolskaya	81	12	7	0	0.9	7.2	0.9	76.5	446	5.1	202	207.1	MFS	MFS	TST	Kashirian
$1k_8$ Nov	Novogrodovskaya	81	14	5	20	0.62	32.6	2.6	53.1	429	15.5	282	297.5	MFS	MFS	TST	Kashirian
$1k_7$ Dim	Dimitrova	77	10	13	5	0.89	11.4	2.7	73.4	440	5.9	233	238.9	TST	TST	TST	Kashirian
$1k_7$ Cen	Centralnaya	84	6	10	0	0.91	1.5	0.9	83.0	446	11	212	223	TST	TST	TST	Kashirian
$3k_5$ Krasno	Krasnolimanskaya	85	9	6	0	0.88	2.4	0.8	84.5	451	11.7	209	220.7	TST	TST	TST	Kashirian
$2k_2^2$ Ka	Kalinina	85	12	3	2	1.03	2.9	0.7	90.7	468	2.4	156.6	259	MFS	MFS	LST	Vereian
$1k_2^2$ Ka	Kalinina	40	58	2	2	1.04	5.5	1.7	84.5	464	1.3	94.7	96	MFS	MFS	LST	Vereian
k_{2u} M 1859	M 1859 borehole	84	16	0	15	1.04								MFS	MFS	LST	Vereian
$3h_{10}$ Pe	Petrovskaya	61	28	11	2	0.63	1.7	1.9	80.4	438	20	243	263	HST	HST	HST	Bashkirian
$2h_{10}$ Pe	Petrovskaya	62	15	23	7	0.62	11.2	2.8	70.6	441	22.8	304	327.2	HST	HST	HST	Bashkirian
$1h_8$ Pe	Petrovskaya	59	21	20	4	0.73	14.9	4.7	67.4	443	21.1	259	280.1	MFS	MFS	HST	Bashkirian
h_8 Glub	Glubokaya	92	8	0	1	1.59	2.0	0.7	89.8	511	16.7	52	69	MFS	MFS	HST	Bashkirian
h_8 Sha Glub	Shakhterskaya Glubokaya	100	0	0	0	4			89.2	671	0.42	3	3.42	MFS	MFS	HST	Bashkirian
d_4 Krw	Krasnoarmeisk Zapadnaya # 1	97	2	1	0	0.92	2.1	0.8	84.5	460	6.8	191	197.8	HST	MFS	HST	Serpukhovian
c_{11} YD	Yuzhno-Donbasskaya # 3	56	29	15	0	0.7	1.9	3.1	81.4	436	6.9	249	255.9	HST	HST	TST	Serpukhovian
$2c_{10}$ YD	Yuzhno-Donbasskaya # 1	59	21	20	2	0.62	2.2	1.8	81.2	430	4.8	260	264.8	HST	HST	TST	Serpukhovian
$1c_{10}$ YD	Yuzhno-Donbasskaya # 1	58	16	26	1	0.63	5.1	4.2	73.7	431	4.9	229	233.9	HST	HST	TST	Serpukhovian

Vitr.: vitrinite; Inert.: inertinite; Lipt.: liptinite; Min. Mat.: mineral matter; Vitr. Refl.: vitrinite reflectance; TOC: total organic carbon content; BI: bitumen index; HI: hydrogen index and QI: quality index. FOS: fourth order sequences, TOS : third order sequences, SOS: second order sequences, LST: lowstand systems tract, TST: transgressive systems tract, MFS: maximum flooding surface and HST: highstand systems tract. Each coal sample is represented in table 1 by its sample code (e.g. $1n_1$ But), that contains a number (1, only in cases were several samples have been taken along a vertical seam section), the name of the coal seam (n_1), and the name of the coal mine (But for Butovskaya).

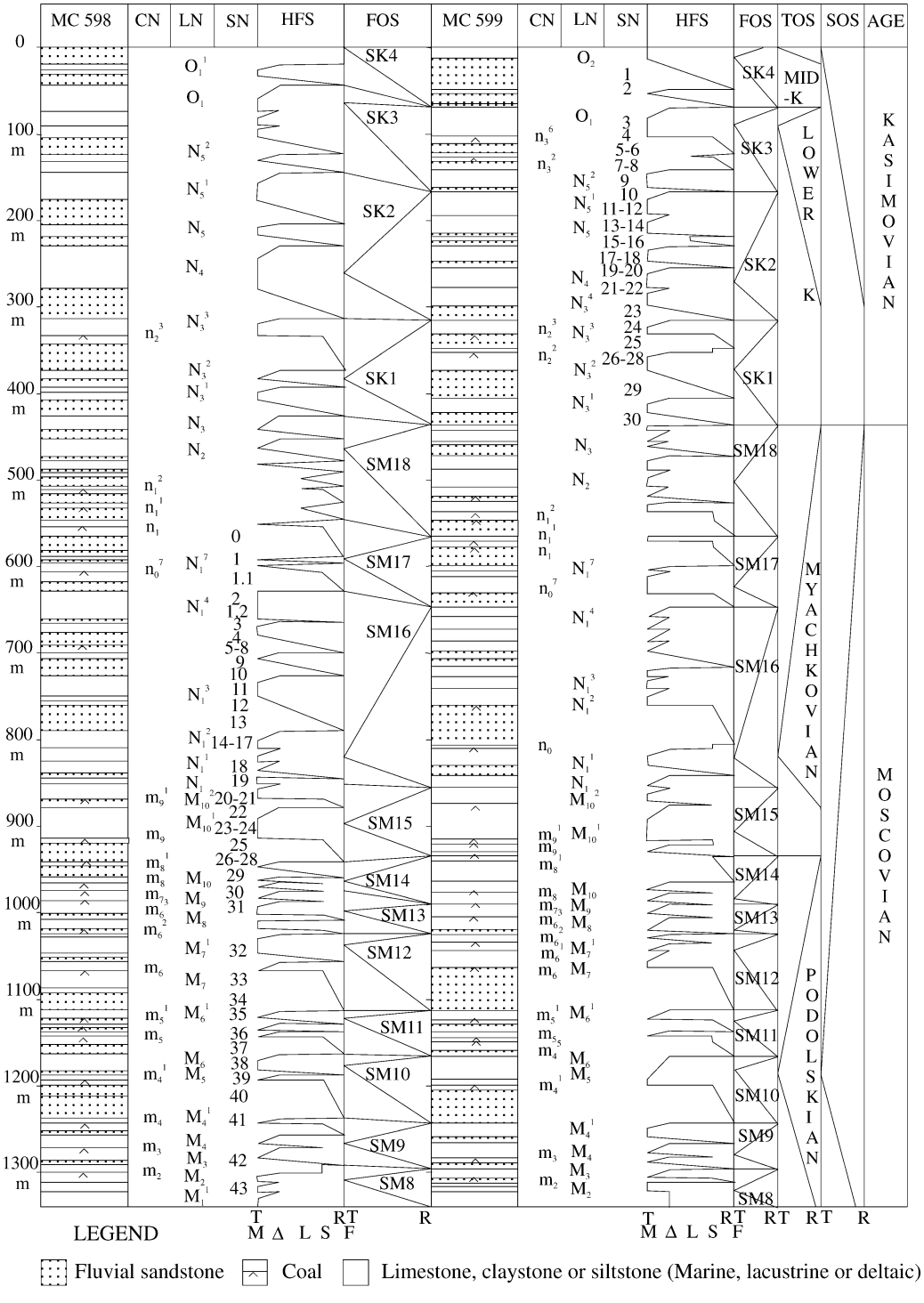
MC 598
CN
LN
SN
HFS
FOS
MC 599
TOS
SOS
AGE
0
100 m
200 m
300 m
400 m
500 m
600 m
700 m
800 m
900 m
1000 m
1100 m
1200 m
1300 m
SK4
SK3
SK2
SK1
SM18
SM17
SM16
SM15
SM14
SM13
SM12
SM11
SM10
SM9
SM8
MID-K
LOWER K
MYACHKOVIAN
PODOLSKIAN
KASIMOVIAN
MOSCOVIAN
T
RT
R
LEGEND
Fluvial sandstone
Coal
Limestone, claystone or siltstone (Marine, lacustrine or deltaic)

4.2. Rock Eval pyrolysis

Bitumen index (BI), quality index (QI) and hydrogen index (HI) are plotted versus T_{max} in Fig. 6. The BI (Fig. 6a) increase up to a VR of 0.8% R_r and a T_{max} of 445 °C, and decreases with higher maturity. The QI (Fig. 6b) and HI (Fig. 6c) decrease progressively with increasing maturity. Most samples follow the trend defined by Sykes and Snowdon (2002). A few samples plot outside the trend. These samples include 5 m_3 Baz (1.2% R_r) and h_8 Glub (1.6% R_r), which have migrated bitumen and, consequently, a high BI value. Low-rank coal o_2 Svet (0.48% R_r) has an unusually low HI and a relatively high T_{max}. A rather high water content (10.9%) suggests that this surface sample is slightly weathered.

4.3. Extract yields and distribution of polars, aromatics and aliphatics

Extract yields range from 0.9 to 66.2 mg/g for coals (Fig. 5b, Table 2) and from 0.01 to 0.65 mg/g for clastics and limestones (Table 3). High values for coals correspond to low-rank (0.4–0.8% R_r) and low values for coals to high-rank (1.6–4% R_r, Fig. 5b). Extract yields in Donbas coals and clastics are similar with those in the Lorraine (Fleck et al., 2001) and higher than in the Central Asturias coal basins (Piedad-Sánchez et al., 2004).

The extracts of Donbas coals (Fig. 5c, Table 2) contain high amounts of polars (34–98%), medium amounts of aromatics (1–58%), and low amounts of aliphatics (2–28%). Asphaltenes represent 2–73% of the extractable organic matter. The percentages of the different fractions are very poorly correlated with VR. Aromatics show a maximum in the maturity range of 0.8% to 1.0% R_r (Fig. 5c). The extracts of Donbas clastics and limestones (Table 3) contain also high amounts of asphaltene+resin fractions (28–74%), medium amounts of aromatics (19–56%), and low amounts of aliphatics (4–25%). Percentages of aromatics and aliphatics are higher in the Donbas than in the Lorraine coal Basin (Fleck et al., 2001).

4.4. Aliphatics

4.4.1. n-Alkanes distributions

The *n*-alkane distributions (m/z 57, Sachsenhofer et al., 2003, Fig. 14) are generally unimodal with maximum peaks between *n*-C_{14} and *n*-C_{19} or *n*-C_{21}. The abundance of longer chain *n*-alkanes decreases exponentially towards *n*-C_{34}.

The samples o_2 Svet, n_3^6 MC, n_3^2 MC, $8l_1$ Dim, h_{10} Pe, and h_8 Pe exhibit a bimodal distribution with a maximum between *n*-C_{14} and *n*-C_{19} and another one between *n*-C_{23} and *n*-C_{31}. In the Lorraine coal Basin (Fleck et al., 2001) two distributions were also observed in coals: light *n*-alkanes from C_{14} to C_{20} and heavy *n*-alkanes from C_{21} to C_{31}.

In Donbas coals, short-chain ($C_{17–19}$) *n*-alkanes (A, Table 2) represent 9% to 56% of all *n*-alkanes. Their percentage increases with rank up to a VR of 0.9% R_r (R^2: 0.25; Fig. 5d). Long-chain ($C_{25–34}$) *n*-alkanes (C: 10–62%) show an opposite trend (Fig. 5e), with the highest proportions of long-chain *n*-alkanes occurring in samples with a bimodal *n*-alkanes distribution. In Donbas clastics and limestones, short-chain ($C_{17–19}$) *n*-alkanes (A, Table 3) represent 19% to 56% of all *n*-alkanes, mid-chain ($C_{20–24}$) *n*-alkanes (B) 27% to 54%, and long-chain ($C_{25–34}$) *n*-alkanes (C) 17% to 52%.

The CPI (carbon preference index) of Donbas coals (Table 2) ranges from 1 to 2. There is only a general trend of decreasing CPI with increasing VR (R^2: 0.04). The CPI of Donbas clastics and limestones (Table 3) ranges from 0.6 to 1.5, generally without a well-marked predominance of odd over even *n*-alkanes.

4.4.2. Isoprenoids

Pristane (Pr) and Phytane (Ph) isoprenoids can be assigned from m/z 57 mass chromatograms. The Pr/Ph ratio of Donbas coals (Table 2) ranges from 1 to 22, and of Donbas clastics and limestones (Table 3) from 0.2 to 8.4. According to Didyk et al. (1978) high ratios indicate dysoxic to oxic conditions, and low ratio reduced conditions. However, Pr/Ph ratios are

Fig. 3. Stratigraphy and sequences of MC598 and MC599 boreholes CN: coal number, D: deltaic paleoenvironment, F: fluvial paleoenvironment, FOS: fourth order sequence, HFS: high frequency sequence, L: lacustrine paleoenvironment, LN: marine band number, M: marine paleoenvironment, *R*: regression, S: swampy paleoenvironment, SK1 to SK4: number of Kasimovian FOS, SOS: second order sequence, SM8 to SM18: number of Moscovian FOS, SN: sample number, *T*: transgression, TOS: third order sequence.

Table 2
Biomarkers data of Donbas coals

Samples	Extr. (mg/g)	Polars (%)	Asph (%)	Aro (%)	Aliph (%)	CPI	A (%)	B (%)	C (%)	Pr/Ph	Pr/ n-C_{17}	Ph/ n-C_{18}	R_{dit}	Hopanes/ steranes	Steranes			MPI1	AGE
															% C_{27}	% C_{28}	% C_{29}		
p_5 Lug	12.7	47	15	32	21	1.38	40	41	19	3.8	5.2	1.9	1.3	15.3	24	34	42	0.48	Gzhelian
o_2 Svet	39.8	98	73	1	2	1.22	18	35	47	4.9	7.9	1.9	1.1	11.1	12	37	51	0.16	Kasimovian
n_3^6 MC 599	23.9	59	16	32	9	1.15	10	28	62	8.9	ND	1.4	1.0	12.0	24	28	48	0.56	Kasimovian
n_2^3 MC 599	15.1	54	7	39	7	1.21	12	26	62	7.3	ND	1.3	2.2	10.0	25	25	50	0.42	Kasimovian
n_2^2 MC 599	8.0	47		45	8	1.17	49	30	31	ND	ND	1.0	2.2	11.8	19	28	53	0.37	Kasimovian
$5n_1$ But	7.0	55	37	37	8	1.22	41	42	17	9.3	10.8	1.1	1.1	18.4	38	15	47	0.32	Myachkovian
$4n_1$ But	11.0	83	42	14	3	1.1	49	37	14	7.6	5.5	0.7	1.5	21.5	28	24	48	0.6	Myachkovian
$3n_1$ But	7.0	66	46	29	5	1.18	55	34	11	7.7	3.4	0.5	1.6	20.8	31	23	46	0.53	Myachkovian
$2n_1$ But	2.7	72	44	22	6	1.15	53	34	13	7.3	4.3	0.6	2.0	22.3	25	26	49	0.62	Myachkovian
$1n_1$ But	2.1	70	41	25	5	1.15	50	33	17	6.9	3.1	0.5	1.7	17.7	26	28	46	0.6	Myachkovian
n_1 But Mak	4.9	94	53	1	5	1.1	27	39	35	1.0	0.7	0.6	1.8	8.9	22	28	50	0.85	Myachkovian
$2m_9$ MC 598	31.9	73	49	23	4	1.09	34	30	36	2.7	0.2	0.3	1.4	8.9	27	29	44	0.51	Myachkovian
$1m_9$ MC 598	40.5	80	63	15	5	1.05	14	38	48	7.3	ND	0.6	1.3	6.2	22	33	45	0.53	Myachkovian
m_8^1 Sch 1355	42.5	73	46	23	4	1.08	34	30	36	0.4	0.1	0.5	1.3	9.4	23	31	46	0.54	Podolskian
m_7 MC 598	44.1	71	44	25	4	1.08	34	29	37	1.0	0.2	0.6	1.2	6.9	22	32	46	0.53	Podolskian
m_6^3 Sch 1355	66.2	85	74	13	2	1.07	18	39	42	6.7	ND	0.5	1.2	3.5	26	33	41	0.48	Podolskian
$2m_5$ Alm	7.2	63	33	30	7	1.11	28	34	38	9.8	19.6	1.9	1.3	22.1	27	30	43	0.39	Podolskian
$4m_4$ Dob	34.0	57	29	32	11	1.3	44	40	16	6.9	3.5	0.6	1.2	19.8	35	31	34	0.7	Podolskian
m_3 Trudo	7.2	55	28	31	14	1.5	28	44	28	5.5	7.3	1.6	1.7	0.5	42	42	16	0.52	Podolskian
m_3 Za	42.8	35	2	58	7	1.08	40	36	25	3.2	1.4	0.5	1.4	2.2	29	34	37	0.7	Podolskian
$1m_2$ Bel	6.7	60	45	34	6	1.15	42	38	20	9.0	13.3	1.6	1.2	11.5	45	22	33	0.62	Podolskian
$1l_8$ Bel	5.0	75	51	20	5	1.16	50	38	12	9.2	7.2	0.9	1.5	11.7	33	27	40	0.75	Podolskian
l_4 Trudo	4.3	58	26	32	10	1.43	29	39	32	10.6	14.0	1.6	1.0	9.5	30	33	37	0.23	Kashirian
$8l_3$ Alm	3.9	67	43	24	9	1.14	52	38	10	6.2	3.3	0.6	1.2	21.6	30	31	39	0.8	Kashirian
$1l_3$ Bel	4.6	72	52	24	4	1.62	56	34	10	8.1	5.3	0.7	1.3	19.9	28	25	47	0.46	Kashirian

$3l_1$ Nov	10.0	52	30	39	9	1.14	53	36	12	8.3	5.3	0.6	1.6	19.2	35	18	47	0.47	Kashirian
$1l_1$ Dob	3.4	59	40	31	10	1.11	53	35	12	6.6	3.7	0.6	1.4	9.3	29	38	33	0.31	Kashirian
$9l_1$ Dim	4.0	66	41	28	6	1.1	45	37	18	6.0	5.4	0.9	1.2	8.1	47	25	28	0.33	Kashirian
$8l_1$ Dim	8.2	80	34	14	6	1.03	23	31	46	6.2	5.8	1.0	1.2	9.0	43	25	32	0.29	Kashirian
$6l_1$ Dim	22.1	70	49	25	5	1.19	35	41	25	6.6	4.5	0.7	1.2	9.2	41	26	33	0.3	Kashirian
$5l_1$ Dim	6.4	68	46	26	6	1.16	47	36	18	7.6	5.8	0.8	1.0	14.6	38	16	46	0.32	Kashirian
$4l_1$ Dim	2.9	63	41	31	6	1.1	51	32	17	7.2	4.3	0.7	1.2	9.0	36	31	33	0.3	Kashirian
$3l_1$ Dim	1.5	61	41	30	9	1.1	37	42	21	5.8	5.6	0.8	1.2	14.7	42	16	42	0.34	Kashirian
$2l_1$ Dim	2.8	67	48	27	6	1.15	36	45	19	5.2	6.1	0.8	1.1	13.0	43	21	36	0.32	Kashirian
$1l_1$ Dim	2.0	68	51	25	7	1.1	50	36	15	6.6	6.1	1.0	1.4	14.3	42	16	42	0.28	Kashirian
$1k_8$ Dob	5.2	63	33	31	6	1.39	35	40	25	6.4	5.9	0.9	1.1	23.7	24	29	47	0.64	Kashirian
$1k_8$ Nov	5.9	76	61	19	5	1.17	35	44	21	4.2	7.6	1.3	1.2	6.3	56	19	25	0.3	Kashirian
$1k_7$ Dim	4.9	68	32	26	6	1.1	48	39	13	7.8	6.3	0.7	1.2	24.2	29	25	46	0.33	Kashirian
$1k_7$ Cen	5.1	68	45	24	8	1.04	38	41	22	6.2	4.2	0.6	1.4	24.2	27	22	51	0.49	Kashirian
$3k_5$ Krasno	4.4	63	50	24	13	1.98	45	44	11	4.4	0.6	0.2	1.0	5.5	26	31	43	0.23	Kashirian
$2k_2^2$ Ka	8.3	35	3	52	13	1.07	46	38	17	2.2	0.5	0.3	0.7	1.3	30	28	42	1.03	Vereian
$1k_2^2$ Ka	18.3	34	8	58	9	1.05	40	42	18	2.0	0.7	0.3	0.7	1.1	24	27	49	1.1	Vereian
k_2u M 1859	29.6	52	27	38	10	1.08	34	38	28	2.2	0.9	0.4	1.0	0.8	22	34	44	0.82	Vereian
$3h_{10}$ Pe	26.5	39	4	39	22	1.42	9	34	58	7.5	ND	0.8	1.6	11.2	39	26	35	0.32	Bashkirian
$2h_{10}$ Pe	33.6	52	23	36	12	1.19	15	35	51	7.9	ND	0.7	1.3	17.9	33	25	42	0.32	Bashkirian
$1h_8$ Pe	11.7	38	20	48	14	1.13	14	34	52	8.1	ND	0.6	1.1	17.1	34	22	44	0.51	Bashkirian
h_8 Glub	1.0	52	26	40	8	1.34	34	41	25	3.4	4.5	1.3	1.6	14.0	25	36	39	0.95	Bashkirian
h_8 Sha Glub	1.0	58	0	14	28	1	24	21	55	3.5	0.2	0.2	1.1	6.4	31	25	44	ND	Bashkirian
d_4 Krw	2.6	64	38	28	8	1.16	50	40	10	3.7	0.6	0.2	1.0	1.5	31	32	37	0.64	Serpukhovian
c_{11} YD	8.6	54	29	34	12	1.24	19	49	33	5.9	10.5	1.0	0.8	17.5	37	29	34	0.51	Serpukhovian
$2c_{10}$ YD	30.9	72	44	24	4	1.32	11	41	48	21.9	ND	0.3	1.1	38.0	19	32	49	0.35	Serpukhovian
$1c_{10}$ YD	7.7	51	25	38	11	1.56	41	45	14	9.5	3.8	0.4	1.2	30.6	30	31	39	0.54	Serpukhovian

Extr.: extract yields; Polars; Asph: asphaltenes; Aro: Aromatics, Aliph: Aliphatics; CPI: carbon preference index; A: $C_{17–19}$ *n*-alkanes; B: $C_{20–24}$ *n*-alkanes; C: $C_{25–34}$ *n*-alkanes; Pr/Ph: pristane/phytane ratio; Pr/*n*-C_{17}: pristane/C_{17} *n*-alkane ratio; Ph/*n*-C_{18}:phytane/C_{18} *n*-alkane ratio; R_{dit}: diterpanes ratio; % C_{27}, C_{28} and C_{29} Steranes; MPI1: methylphenantrene index.

Table 3
Biomarkers data of Donbas clastics and limestones

Samples	Strat	Lithology	Environment	Vitr. Refl. (% Rr)	Extr. (mg/g)	Polars (%)	Asph (%)	Aro (%)	Aliph (%)	CPI	A (%)	B (%)	C (%)	Pr/Ph	Pr/*n*-C17	Ph/*n*-C18	R_{dit}	Hopanes/ steranes	Steranes			MPI1	HFS
																			% C_{27}	% C_{28}	% C_{29}		
MC599-1	Ka	siltstone	levee	0.62	0.12	49		35	16	1.2	25	33	42	1.89	1.75	0.8	1.5	9.86	25.29	28.25	46.45	0.33	LST
MC599-3-O_1		claystone	sea		0.075	46		30	24	1.16	32	35	33	1.42	1.24	1	1.2	9.69	34.25	25.37	40.37	0.26	MFS
MC599-4		limestone	sea		0.037	52		28	20	0.8	31	34	35	0.9	2.3	0.7	0.9	1.9	26	24	50		TST
MC599-n_3^6		coal	swamp	0.63	23.9	59	16	32	9	1.15	10	28	62	8.9	nd	1.4	1	12	24	28	48	0.56	TST
MC599-5		siltstone	delta		0.05	46		29	25	0.7	53	27	20	0.7	1	1.2	0.8	3.6	26	28	46		HST
MC599-6		claystone	lake		0.05	57		30	13	0.7	48	29	23	0.7	0.7	0.9	0.7	9.9	21	25	54		TST
MC599-8		siltstone	levee	0.64	0.1	61		27	13	1.46	35	32	33	1.53	1.34	0.78	1	2.32	28.06	25.87	46.06	0.3	LST
MC599-10		claystone	lake	0.64	0.1	48		34	18	1.24	35	34	31	1.09	1.15	1.06	1.1	5	24.85	29.62	45.13	0.17	MFS
MC599-13-N_5^1		claystone	sea		0.06	64		23	13	1.35	51	27	22	1.06	0.66	0.81	1.3	14.83	51.34	21.8	28.85	0.32	MFS
MC599-16		sandstone	river		0.1	53		32	15	1.22	45	31	24	1.22	0.85	0.87	1.5	3.88	29.25	28.35	42.4	0.3	LST
MC599-19		claystone	lake	0.67	0.8	45		45	10	1.26	43	28	29	nd	nd	0.68	0.3	5.19	17.93	26.21	55.85	0.33	MFS
MC599-22		siltstone	delta	0.67	0.29	49		38	13	1.22	36	31	33	2.08	1.1	0.7	1.3	6.68	22.35	26.79	50.85	0.2	HST
MC599-24-N_3^3		claystone	sea		0.08	49		31	20	1.39	29	36	35	1.22	0.96	0.82	1.4	14.11	31.92	27.55	40.52	0.39	MFS
MC599-n_2^3		coal	swamp	0.65	15.1	54	7	39	7	1.21	12	26	62	7.3	nd	1.3	2.2	10	25	25	50	0.42	TST
MC599-26		siltstone	delta		0.02	56		34	10	0.7	36	39	25	0.3	0.8	0.7	1.5	7.9	57	14	29		HST
MC599-27-n_2^2		coal	swamp	0.7	8	47		45	8	1.17	49	30	31	nd	nd	1	2.2	11.79	18.47	28.21	53.31	0.37	TST
MC599-28-N_3^2	Ka	claystone	sea		0.29	40		48	12	1.14	36	34	30	nd	nd	1.24	2.3	2.05	30.7	18.64	50.64	0.35	MFS
$2n_1$ But	Mya	coal	swamp	0.83	2.7	72	44	22	6	1.15	53	34	13	7.3	4.3	0.6	2	22.3	25	26	49	0.62	TST
MC598-1		sandstone	fluvial		0.02	56		33	11	0.6	29	33	38	1.8	1.3	0.2							LST
MC598-8		siltstone	levee		0.04	59		32	9	1	43	40	17	1	1.5	0.6	1.1	9.5	20	31	49		LST
MC598-11		siltstone	delta	0.83	0.22	49		41	10	1.21	30	36	34	2.66	0.97	0.35	1.3	12.35	31.72	17.9	50.38	0.48	HST
MC598-14-N_1^2		claystone	sea		0.16	51		38	11	1.2	21	38	41	2.13	1.42	0.61	0.9	18.08	40.76	13.92	45.32	0.5	MFS
MC598-15		siltstone	levee		0.02	53		25	22	1	29	47	24	0.4	0.8	0.3	1	5.6	26	25	49		LST
MC598-17		claystone	sea		0.04	58		31	11	0.9	31	40	29	1	1	0.5	0.5	16.5	26	25	49		TST

MC598-19-N_1		claystone	sea		0.07	51		33	16	1.12	20	28	52	1.18	0.62	0.52	1.9	7.88	42.51	23.37	34.12	0.22	MFS
MC598-20		siltstone	delta	0.83	0.15	74		19	7	1.26	24	36	40	3.49	1.23	0.37	1.4	7.06	42.78	23.08	34.14	0.46	HST
MC598-21-M^2_{10}		claystone	sea		0.09	46		31	23	1.17	31	38	31	2.09	0.75	0.37	1.2	5.88	41.18	23.49	35.33	0.39	MFS
MC598-22		claystone	delta		0.12	57		31	12	1.18	21	37	42	1.28	1.39	0.81	1.2	12.78	35.32	20.48	44.2	0.29	HST
MC598-23		siltstone	delta		0.1	53		37	10	0.9	38	36	26	0.8	1	0.5	0.9	11.4	54	15	31		HST
MC598-24		claystone	sea		0.06	61		32	7	0.9	28	38	34	0.9	1.2	0.7	0.6	7.9	56	16	28		TST
MC598-2m_9		coal	swamp	0.8	45.5	73	49	23	4	1.09	34	30	36	2.68	0.22	0.28	1.4	8.88	27.57	29.82	44.61	0.51	TST
MC598-1m_9		coal	swamp	0.78	57.9	80	63	15	5	1.05	14	38	48	7.33	nd	0.6	1.3	6.22	22.49	32.76	44.75	0.53	TST
Sch-1355-m^1_8	Mya	coal	swamp	0.83	60.7	73	46	23	4	1.08	34	30	36	0.35	0.05	0.53	1.3	9.37	22.93	30.95	46.12	0.54	TST
MC598-30-m_{10}	Pod	claystone	sea		0.27	35		41	24	1.03	35	36	29	1.4	0.52	0.41	0.7	2.21	53.99	15.26	30.75	0.53	MFS
MC-598-m_7		coal	swamp	0.79	63	71	44	25	4	1.08	34	29	37	0.98	0.16	0.59	1.2	6.94	22.58	31.41	46.01	0.53	TST
Sch-1355-m^3_6		coal	swamp	0.76	94.5	85	74	13	2	1.07	18	39	42	6.71	nd	0.52	1.2	3.5	26.42	32.79	40.79	0.48	TST
MC598-31		siltstone	delta		0.02	56		29	15	0.6	18	42	40	0.2	0.8	0.6	0.6	5.2	21	28	51		HST
MC598-32		siltstone	delta		0.13	48		29	23	0.9	15	54	31	8.4	2	0.2	1	2.3	29	34	37		HST
MC598-35		claystone	delta		0.11	51		45	4	0.9	22	39	39	0.5	0.9	0.6	0.8	3.5	27	27	46		HST
MC598-36		claystone	lake	0.9	0.18	43		44	13	1.09	30	37	33	1.79	0.46	0.26	1.4	4.34	29.98	20.24	49.78	0.6	MFS
2m_5Alm		coal	swamp	0.73	7.2	63	33	30	7	1.11	28	34	38	9.8	19.6	1.9	1.3	22.1	27	30	43	0.39	TST
MC598-38		siltstone	delta	0.92	2.4	35		56	9	1.32	40	40	20	2.3	0.5	0.3	1.2	4.72	20.28	28.72	51	0.54	HST
MC598-39		limestone	sea		0.02	51		37	12	1	15	38	47	0.6	1	0.4	0.3	2.7	29	24	47		TST
MC598-41		siltstone	delta	0.99	0.21	44		45	11	1.39	34	39	27	1.47	0.43	0.33	1.2	2.56	36.47	23.78	39.7	0.29	HST
4m_4Dob		coal	swamp	0.7	34	57	29	32	11	1.3	44	40	16	5.5	3.5	0.6	1.2	19.8	35	31	34	0.7	TST
m_3Trudo		coal	swamp	0.39	7.2	55	28	31	14	1.5	28	44	28	3.2	7.3	1.6	1.7	0.5	42	42	16	0.52	TST
MC598-42		limestone	sea		0.01	51		25	24	0.9	20	35	45	0.5	1	0.7	0.5	1	57	17	26		TST
1m_2Bel		coal	samp	0.71	6.7	60	45	34	6	1.15	42	38	20	9	13.3	1.6	1.2	11.5	45	22	33	0.62	TST
MC598-43-m_2	Pod	claystone	sea		0.65	28		52	20	1	25	34	41	0.86	0.42	0.65	1	1.29	40.73	28.4	30.87	0.6	MFS

known to be affected by differences in the nature of the contributing sources (Volkman and Maxwell, 1986; ten Haven et al., 1987) and by maturation (Tissot and Welte, 1984; Koopmans et al., 1999). The latter is also supported by Fig. 5f, which shows that Pr/Ph ratios from coals exhibit a maximum in samples with a VR close to 0.7% R_r ($2m_5$ Alm, l_4 Trudo, $1l_8$ Bel, $1c_{10}$ YD), whereas low values were observed in low and high-rank coals. Therefore, Pr/Ph ratios are interpreted with great caution.

The Pr/*n*-C_{17} ratio ranges from 0.2 to 20 for Donbas coals (Table 2) and from 0.4 to 2.3 for Donbas clastics and limestones (Table 3). The Ph/*n*-C_{18} ratio ranges from 0.2 to 1.9 for Donbas coals (Table 2) and from 0.2 to 1.3 for Donbas clastics and limestones (Table 3). After Lijmbach (1975), these ratio change versus continental and marine environments.

4.4.3. Diterpanes

Diterpanes are recognized from the m/z 123 mass chromatograms (Fig. 7 and Table 4). The determination was made by comparing chromatograms and mass spectra with data from Noble et al. (1985a,b). After Fleck (2001), the R_{dit} ratio=(19-Norisopimarane+*iso*-Pimarane+16α-Kaurane)/(*ent*-Beyerane+16β-Phyllocladane+16α-Phyllocladane) was calculated and ranges from 0.7 to 2.2 for Donbas coals (Table 2) and from 0.3 to 2.3 for Donbas clastics and limestones (Table 3). There is no correlation between R_{dit} from coals and VR (Fig. 5g). R_{dit} is maximum in coals and minimum in marine limestone.

The samples were classified into three groups according to the relative proportions of diterpanes and R_{dit}:

- group 1 with 5 (β-Phyllocladane)>6 (Kaurane)>3 (*ent*-Beyerane) or 6>5>3 or 6>5>7 (α-Phyllocladane), 3>5>6 and R_{dit}< 1.1. This group comprises Kasimovian (o_2, n_3^6), Kashirian (l_4, k_5), Vereian (k_2, k_2^2), Bashkirian (h_8), and Serpukhovian (d_4, c_{10}, c_{11}) coals, deltaic siltstones, limestones, and marine or lacustrine claystones;
- group 2 with 4 (*iso*-Pimarane)>6>3, 6>5>7, 6>5>4, 6>2>3 or 2>3>4 and R_{dit}>1.5 for lower part of Kasimovian (n_2^3, n_2^2), Myachkovian (1-4n_1 But), Podolskian (m_3), Kashirian (l_1 Nov), and Bashkirian (h_{10}, h_8) coals, deltaic siltstones, and marine claystones;
- group 3 with 6>3>4 or 6>4>3 or 6>3>5 or 6>3>7 or 6>5>3 or 6>7>3 and R_{dit}=1.1 to 1.5 comprising Gzhelian (p_5), Myachkovian ($5n_1$ But, m_9, m_8^1), Podolskian (m_7 to m_2), Kashirian (l_8, l_3, l_1, k_8, k_7), Bashkirian (h_{10}), and Serpukhovian (c_{10}) coals, fluvial sandstone, levee and deltaic siltstones, limestones, and marine or lacustrine claystones.

R_{dit} is low (0.78) to intermediate in Serpukhovian coals, and high (1.5) in Bashkirian coals. Within the Moscovian sequence the R_{dit} ratio increases upwards from Vereian (0.7) to Myachkovian (1.6) levels and reaches a peak in the lowermost Kasimovian (2.2). Lower values occur in lower Kasimovian (1.1) and Gzhelian (1.3) coals. Vertical variations within single seams (e.g. n_1 But, l_1 Dim) reflect variable contributions to the peat forming vegetation and/or a varying height of the water table.

4.4.4. Steranes

Steranes are recognized from the m/z 217 mass chromatograms (Fig. 7 and Table 4). The determination was made by comparing with mass chromatograms and mass spectra in literature (Moldovan et al., 1992; Philp, 1985). Based on sterane carbon number distributions, the Donbas coals (Fig. 8a), limestones and clastic rocks (Fig. 8b) are classified into three groups, subdivided themselves after stratigraphy (Fig. 8a) or lithology (Fig. 8b):

- group 1 with a predominance of C_{29} steranes: C_{29} (39–51%), C_{28} and C_{27} (20–30%). This group comprises Gzhelian (p_5), Kasimovian (o_2, n_3^6, n_2^3, n_2^2), Myachkovian (n_1, m_9, m_8^1), Podolskian (m_7, m_6^3, m_5), Kashirian (l_1, k_8, k_7, k_5), Vereian (k_2, k_2^2), Bashkirian (h_{10}, h_8), Serpukhovian (c_{10}) coals, limestones, marine and lacustrine claystones, levee and deltaic siltstones, and fluvial sandstone (Table 3).
- group 2 with similar proportions of C_{29}, C_{28} and C_{27} steranes comprises Podolskian (m_4, m_3), Kashirian (l_8, l_4, l_3) and Serpukhovian (d_4, c_{10}, c_{11}) coals, marine claystones and deltaic siltstones.
- group 3 with C_{27} or C_{28} equal or higher than C_{29} comprising Podolskian (m_3, m_2) and Kashirian (l_1, k_8) coals, marine limestones and claystones and deltaic siltstones (Table 3).

Table 4
Peak assignments and formula for diterpanes and steranes in Fig. 6 and hopanes

Peak number	Name
Diterpanes (m/z= 123)	
2	19-Norisopimarane
3	ent-Beyerane
4	*iso*-Pimarane
5	16β-Phyllocladane
6	16α-Kaurane
7	16α-Phyllocladane
R_{dit}=(2+4+6)/(3+5+7)	
Steranes (m/z= 217)	
1	14α, 17α-Cholestane(20S) (C_{27})
2	14β, 17β-Cholestane(20R) (C_{27})
3	14β, 17β-Cholestane(20S) (C_{27})
4	14α, 17α-Cholestane(20R) (C_{27})
5	24-Methyl-14α 17α-Cholestane(20S) (C_{28})
6	24-Methyl-14β, 17β-Cholestane(20R) (C_{28})
7	24-Methyl-14β, 17β-Cholestane(20S) (C_{28})
8	24-Methyl-14α, 17α-Cholestane(20R) (C_{28})
9	24-Ethyl-14α, 17α-Cholestane(20S) (C_{29})
10	24-Ethyl-14β, 17β-Cholestane(20R) (C_{29})
11	24-Ethyl-14β, 17β-Cholestane(20S) (C_{29})
12	24-Ethyl-14α, 1-Cholestane(20R) (C_{29})
Steranes=1+2+3+4+5+6+7+8+9+10+11+12	
% C_{27} Steranes=100(1+2+3+4)/Steranes	
% C_{28} Steranes=100(5+6+7+8)/Steranes	
% C_{29} Steranes=100(9+10+11+12)/Steranes	
Hopanes (m/z= 191)	
3	17β(H) 22, 29, 30-Trisnorhopane (C_{27})
4	17α(H), 21β(H)-Norhopane (C_{27})
7	17α(H), 21β(H)-Hopane (C_{30})
10	(22S)17α(H), 21β(H)-Homohopane (C_{31})
11	(22R)17α(H), 21β(H)-Homohopane (C_{31})
13	(22S)17α(H), 21β(H)-Bishomohopane (C_{32})
14	(22R)17α(H), 21β(H)-Bishomohopane (C_{32})
Hopanes=3+4+7+10+11+13+14	
Ho/St=Hopanes/Steranes	

There is no correlation between relative proportions of C_{29}, C_{28} and C_{27} steranes from coals and VR (Fig. 5h–j).

4.4.5. Hopanes

Hopanes are recognized from the m/z 191 mass chromatograms (Table 4, Sachsenhofer et al., 2003, their Fig. 14). The determination was made by comparing chromatograms with data from Moldovan et al. (1992). A unimodal distribution of hopanes with a maximum at C_{30} is found for all samples. The hopanes/steranes ratio of coals (Table 4) ranges from 0.5 to 38 with a mean of 13.3. This ratio is not correlated with rank (Fig. 5k). The hopanes/steranes ratio of limestones and clastics ranges from 1 to 18. The values are minimum in limestones and maximum in coals.

4.5. Aromatics

Phenanthrene, methyl-phenanthrene, and dimethyl-phenanthrene were characterized after full-scan and SIM of m/z 178, 192 and 206. The methyl-phenanthrene index (MPI1) was calculated according to Radke and Welte (1983)

$$\mathrm{MPI1} = 1.5*(\text{2-MP} + \text{3-MP}) / (\mathrm{P} + \text{1-MP} + \text{9-MP})$$

where P = phenanthrene and MP = methyl phenanthrene.

The MPI1 of Donbas coals ranges from 0.15 to 1.1 (Fig. 5l) and increases with rank up to a VR of 1.3% R_r, and decreases in high-rank coals. The trend line (Fig. 5l) is identical with that for Ruhr Basin coals with a VR <1.3% R_r (Radke and Welte, 1983). The MPI1 of Donbas clastics ranges from 0.17 to 0.6.

Naphthalene, methyl-naphthalene, di- and trimethyl-naphthalene, fluoranthene and pyrene, benzofluoranthene, benzo[*e*]pyrene and benzo[*a*]pyrene, chrysene, and retene were recognized in full-scan and SIM (ions 202, 219, 228 and 252). Relatively high proportions of pyrene, benzo[*e*]pyrene, and benzo[*a*]pyrene are observed in samples with inertinite per-

Notes to Table 3:
HFS: high frequency sequences, Ka: Kasimovian, Mya: Myachkovian, Pod: Podolskian, Strat: stratigraphy, and see other legends in Tables 1 and 2.

Table 5
Relationships between macerals, sulphur, biomarkers and eustacy

Sequences		Fourth order seq.(FOS)				Third order seq.(TOS)				Second order seq.(SOS)				High frequency seq.(HFS)				
System tracts		LST	TST	MFS	HST	LST	TST	MFS	HST	LST	TST	MFS	HST	LST	TST1	TST2	MFS	HST
Number of samples		3	18	44	41	5	24	53	24	5	52	15	34					
Vitrinite	Mean %	80	84.2	79.1	77.6	76.4	84.2	78.6	77	70.4	79.3	83	79.3					
	σ %	2.7	4.9	10.8	12.8	6.7	7.5	10.8	14.3	18.8	10	8.2	13.3					
	Max %	82	96	100	100	82	100	98	100	85	98	100	100					
	Min %	77	72	40	52	65	72	40	52	40	52	72	56					
Inertinite	Mean %	12.33	7.7	13.2	13.3	16.4	7.9	13.56	13	26.2	11	10.7	12.9					
	σ %	2.5	4.9	10.1	8.8	7.4	4.9	9.8	9.3	18.9	7.2	6.6	8.8					
	Max %	15	19	58	32	29	19	58	32	58	29	25	32					
	Min %	10	1	0	0	10	0	1	0	12	1	0	0					
Liptinite	Mean %	8	8.2	7.4	9.1	7.2	8	7.6	10	3.4	9.5	6.4	7.8					
	σ %	0	5.3	5	6	1.1	5.2	4.7	7	2.6	5.7	3.8	5.4					
	Max %	8	23	23	26	8	23	23	26	6	26	17	23					
	Min %	8	2	0	0	6	0	0	0	0	0	0	0					
Vitrinite/	Mean	0.87	0.91	0.85	0.85	0.82	0.91	0.85	0.85	0.73	0.87	0.88	0.86					
(Vitr.+Inert.)	σ	0.03	0.05	0.11	0.1	0.08	0.06	0.12	0.12	0.19	0.08	0.07	0.1					
	Max	0.89	0.99	1	1	0.89	1	0.99	1	0.88	0.99	1	1					
	Min	0.84	0.79	0.41	0.64	0.69	0.79	0.41	0.59	0.41	0.66	0.74	0.62					
Number of samples		3	18	52	47	6	24	66	24	5	58	24	34					
Sulphur	Mean	5.23	2.1	2.72	3.5	6.87	2.58	2.77	2.97	6.84	2.53	3.62	2.94					
	σ %	2.94	1.97	2	7.2	4.14	2.34	1.73	2.68	5.4	1.43	2.42	2.71					
	Max %	8.5	7.3	8	13.2	13.2	8	7.4	12.5	13.2	7.4	8	12.5					
	Min %	2.8	0.7	0.4	0.83	2.8	0.4	0.4	0.9	0.7	0.7	0.4	0.4					
Number of samples		3	5	14	28	6	5	24	15	5	22	6	17	6	13	3	15	12
Pristane/	Mean	3.46	5.84	5.43	7.35	4.23	7.44	5.85	8.24	3.4	7.55	7.25	5.64	1.3	5.75	0.64	1.29	2
Phytane	σ	3.51	3.35	2.58	3.3	3	2.16	1.95	4.4	2.6	3.57	2.57	2.66	0.56	3.2	0.2	0.46	2.25

	Max	7.3	9.77	8.99	21.94	7.3	9.77	8.95	21.9	7.3	21.9	9.77	9.31	1.9	9.8	0.87	2.1	8.4
	Min	0.4	1	1.95	3.69	0.4	4.39	1.95	1	1.95	4.13	3.17	0.4	0.4	0.35	0.5	0.7	0.2
R_{dit}	Mean	1.33	1.18	1.16	1.33	1.61	1.16	1.19	1.3	1.36	1.16	1.35	1.35	1.22	1.5	0.56	1.1	1.1
	σ	0.06	0.14	0.27	0.35	0.45	0.14	0.24	0.31	0.78	0.17	0.2	0.26	0.26	0.45	0.31	0.52	0.28
	Max	1.4	1.3	1.69	2.2	2.2	1.3	1.69	1.95	2.2	1.59	1.69	1.95	1.5	2.3	0.9	1.9	1.5
	Min	1.3	0.96	0.66	0.78	1.29	0.96	0.66	0.78	0.66	0.78	1.13	0.95	1	1	0.3	0.3	0.6
Hopanes/	Mean	8.2	16.58	10.67	14.67	10.27	17.5	11.26	17.24	4.95	15.97	11.3	13.16	6.22	11.15	1.87	8.32	6.67
Steranes	σ	1.72	9.52	8.58	7.6	3.05	8.52	6.98	8.98	5.48	8.36	8.83	6.43	3.34	6.73	0.85	5.42	3.75
	Max	9.4	24.2	23.71	38	15.26	24.2	23.71	38	11.8	38	22.1	22.33	9.9	22.3	2.7	18	13
	Min	6.2	5.5	0.49	1.49	6.2	5.5	0.49	3.5	0.8	5.5	0.49	1.49	2.3	0.5	1	1.3	2
C_{27} steranes	Mean %	24	26.41	31.8	32.16	23.27	30.9	35	28.64	23.96	34.43	35	27.29	25.72	27.96	37	36.12	33.57
	σ %	2.64	2.66	9.77	8.65	2.69	7.72	8.55	7.32	3.96	9	7.03	6.47	3.57	7.89	17	11.6	12.24
	Max %	27	29.22	56.16	47.57	27	44.62	56.16	38.87	29.73	56.16	44.62	38.87	29	45	57	54	57
	Min %	22	22	22	12.11	19	26.72	23.55	12.11	19	19	26.84	12.11	20	18.5	29	21	20
C_{28} steranes	Mean %	31	27.73	29.25	26.41	30.17	25.6	26.8	28.17	28.55	25.68	30.7	28.71	27.69	30	22	22.66	23.89
	σ %	2	4.36	6.16	6.35	3.24	4.34	7.22	5.42	3.32	6.18	6.93	5.75	2.36	4.8	4	4.89	6.05
	Max %	33	32	41.86	40.26	34.33	30.87	41.86	36.75	34	37.85	41.86	36.75	31	32.79	24	30	34
	Min %	29	21.54	19.33	26.41	25.67	21.4	15.72	15.08	25	15.72	21.4	15.08	25	22	17	14	14
C_{29} steranes	Mean %	45	45.94	38.94	41.38	46.56	43.5	38.1	43.3	47.49	39.89	34.3	43.98	46.58	42.2	41	41.23	42.52
	σ %	1	3.2	9.35	6.8	4.14	6.23	8.27	5.44	4.53	7.48	9.5	4.25	2.71	9.78	13	9.49	8.12
	Max %	46	51.18	48.71	53.31	53	51.18	48.71	51.13	53	51.18	43.92	51.13	49	53.31	50	56	51
	Min %	44	42.85	16.44	27.92	41.59	33.97	16.44	33.85	41.83	24.5	16.44	34.92	42	16	26	28	29

Mean: average value; mini: minimum value; maxi: maximum value, σ: standard deviation. HFS: high frequency sequences, FOS: fourth order sequences, TOS: third order sequences, SOS: second order sequences, LST: lowstand systems tract, TST1: early transgressive systems tract (coal), TST2: late transgressive systems tract (limestone), MFS: maximum flooding surface and HST: highstand systems tract.

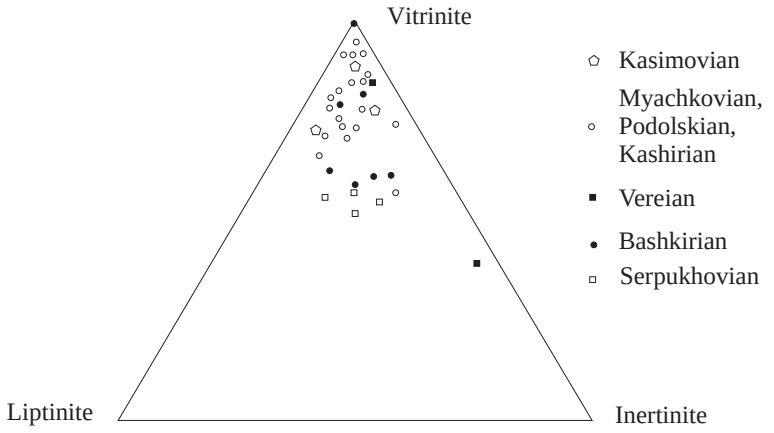

Fig. 4. Comparison of average maceral group percentages in coal seams from Serpukhovian to Kasimovian.

centages higher than 20% ($4n_1$ But, $5l_1$ Dim, $1c_{10}$YD, c_{11}YD).

Aromatized arborane/fernane triterpenoids (Vliex et al., 1994), consisting of monoaromatic tetracyclic hydrocarbons (MATH), monoaromatic pentacyclic hydrocarbons (MAPH), and diaromatic pentacyclic hydrocarbons (DAPH), were only detected in Kasimovian (o_2 Svet) and Gzhelian (p_5 Lug) samples.

5. Discussion

5.1. Thermal maturity

According to the interpretation of Sykes and Snowdon (2002), coals are generally gas and oil-prone (Fig. 6c). All but one sample reached the oil window. Higher rank coals expelled oil or even generated gas (Fig. 6a, b).

The increasing BI values of low-rank coals reflect the progressive transformation of kerogen into free hydrocarbons. The hydrocarbons were not expelled, but are retained within the coal pores. QI and HI of higher rank coals decrease due to expulsion and thermal cracking. The exceptionally high values of BI of the high-rank coals samples $5m_3$ Baz and h_8 Glub are due to migrated bitumen residing within the pores of inertinite macerals. To minimize effects due to maturity and migration, only biomarkers from coal samples with a VR lower or equal to 0.9% R_r were used for paleoenvironmental and paleoclimatic reconstruction. However, samples from Serpukhovian seam d_4 (0.92% R_r) and Vereian seam k_2 (1.04% R_r) were included, because of their special stratigraphic interest.

Liptinite disappears at a VR of 1.4% R_r, and its absence leads to a slightly enrichment in vitrinite in high-rank coals. Many chemical parameters reach a maximum in the maturity range between 0.7% and 0.9% R_r (e.g. extraction yield, aromatics, pristane/phytane ratio). The percentage of short-chain (C_{17-19}) *n*-alkanes increases and the percentage of long-chain (C_{25-34}) *n*-alkanes decreases up to a VR of 0.9% R_r.

These results agree with artificial maturation experiments (Eglinton et al., 1988; Han et al., 2001; Piedad-Sánchez et al., 2005) and with studies in other coal basins. A thermal effect was observed in British coals and in Ruhr Basin coals (Allan and Douglas, 1977; Littke et al., 1989a,b; Radke et al., 1980), where a set of coals with a VR of 0.7%, 0.9% and 1.3% R_r exhibits *n*-alkane maxima at C_{27}, C_{21} and C_{17}, respectively. Radke et al. (1980) showed that in low-rank coals the oxidation, then decarboxylation of phytol results in the generation of pristane and a Pr/Ph maximum at a VR of 0.9% R_r. Recent investigations show that variables sources for pristane and phytane may be considered (Koopmans et al., 1999; Höld et al., 2001 and reference therein). Despite this, Pr/Ph ratio is still used as a redox indicator for the depositional environment. Increasing Pr/Ph ratios during thermal maturation mainly result of higher precursors of Pr (Koopmans et al., 1999). The Pr/Ph ratio decreases in higher-rank coals due to a preferential degradation

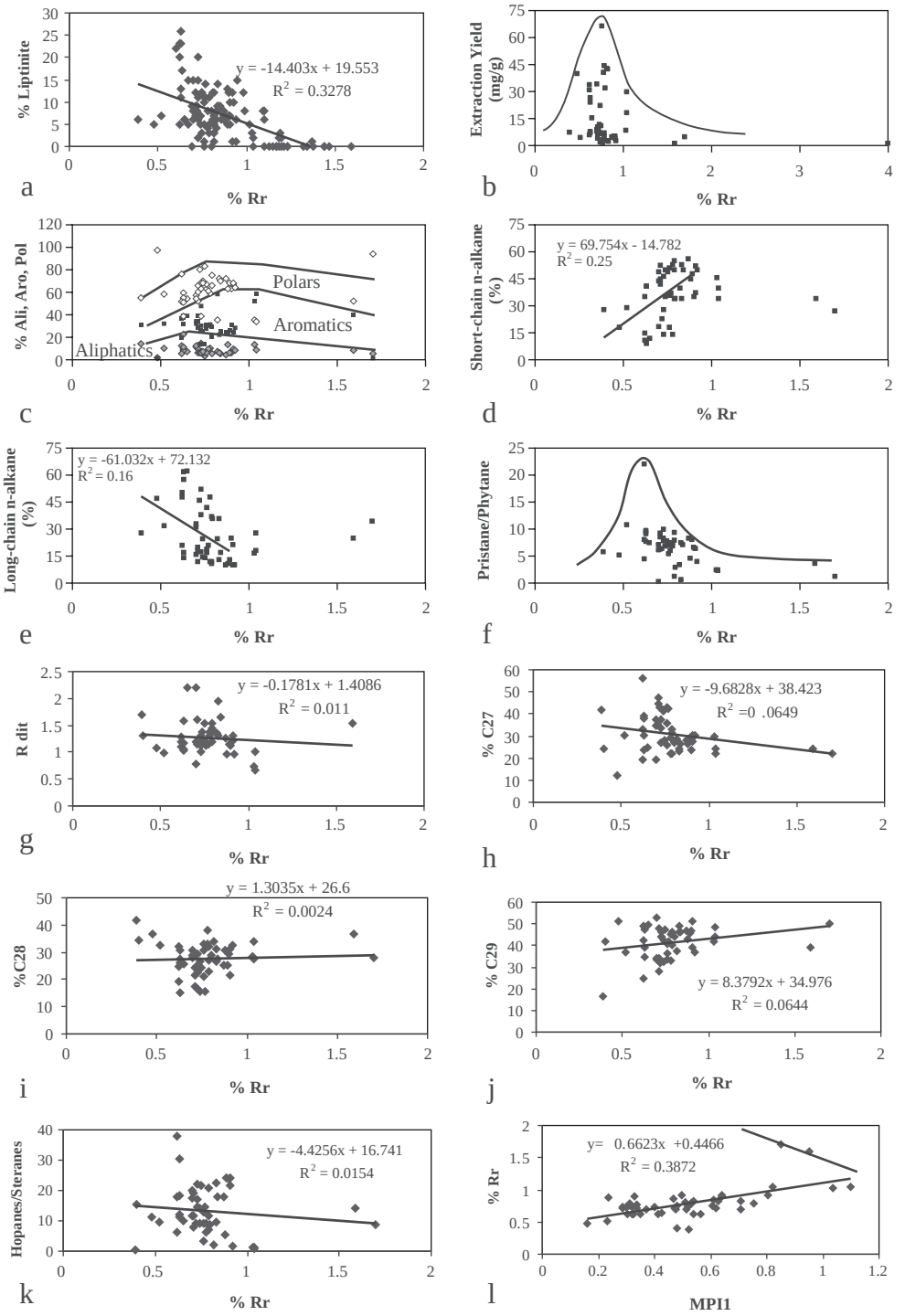

Fig. 5. Maceral and biomarker data versus vitrinite reflectance (% R_r). (a) % liptinite; (b) extraction yield; (c) % aliphatics, aromatics and polars; (d) % short-chain *n*-alkanes; % long-chain *n*-alkanes; (f) Pristane/Phytane; (g) R_{dit}; (h) % C_{27} steranes; (i) % C_{28} steranes; (j) % C_{29} steranes; (k) hopanes/steranes; (l) vitrinite reflectance (% R_r) versus MPI1. Correlation coefficient R^2 and formula are provided for some correlations.

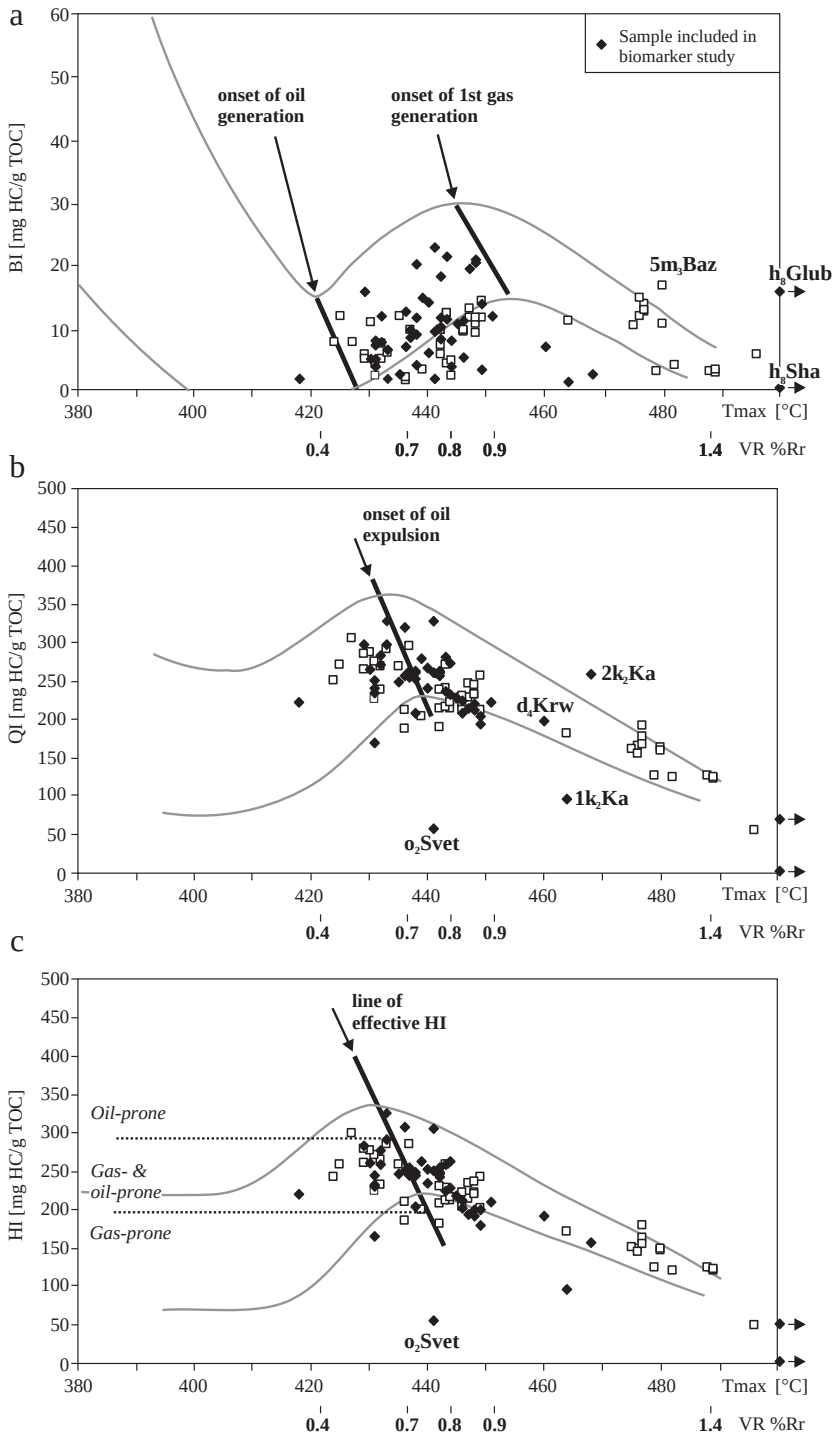

Fig. 6. Rock–Eval indexes. (a) bitumen index (BI), (b) quality index (QI) and (c) hydrogen index (HI) versus T_{max}. Samples included in the biomarker study are shown. Note that high-rank coals h8 Glub and h8 Sha were not used for paleoclimatic interpretations.

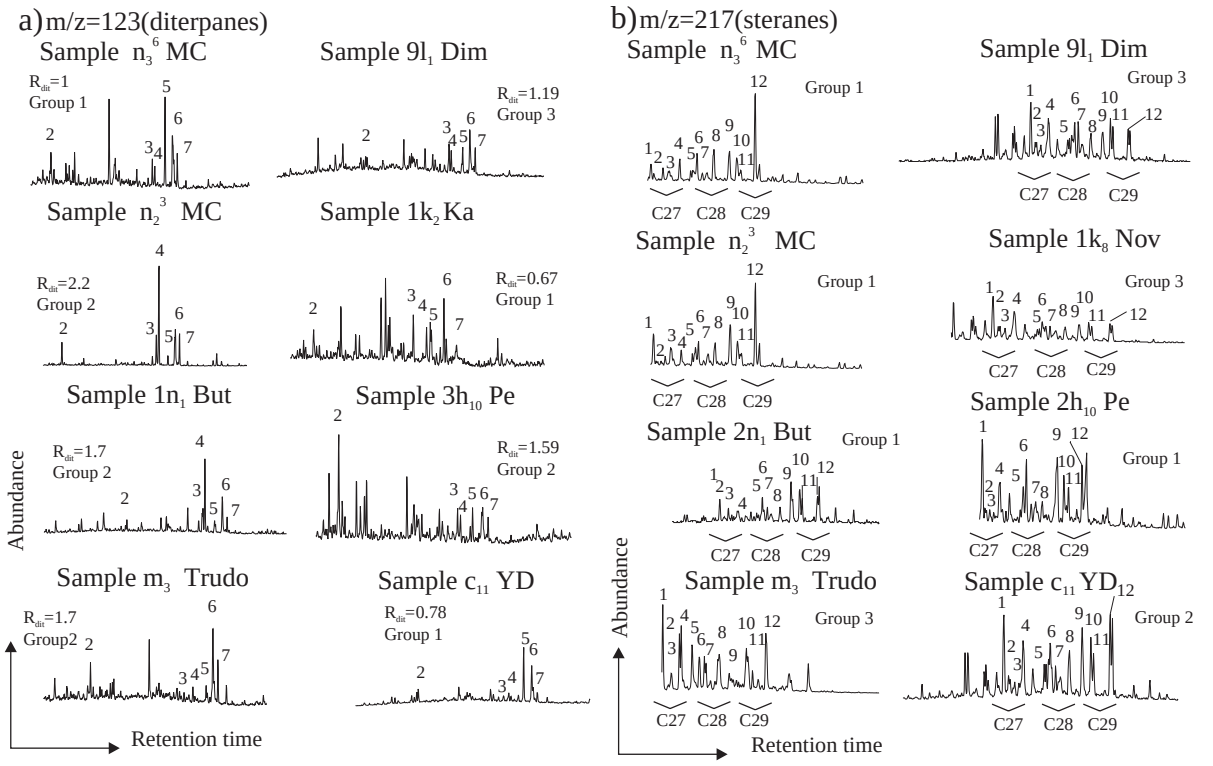

Fig. 7. Examples of (a) diterpane distributions and (b) sterane distributions of typical Donbas coals. Peaks are identified in Table 4. R_{dit} and group of steranes are indicated for each sample.

of pristane compared to phytane. A similar pattern is observed in Donbas coals. The proportion of C_{29}, C_{28} and C_{27} steranes were probably not influenced by maturity because of the generally low rank of the coals (<0.9% R_r). The same applies for diterpanes and hopanes. For higher ranks, Piedad-Sánchez et al. (2005) showed by pyrolysis that proportion of *n*-alkanes, steranes, diterpanes and hopanes change.

5.2. Paleoenvironmental assessment

The relationship between biomarkers and sources of organic matter was already discussed for Donbas (Sachsenhofer et al., 2003) and Asturias coal basin (Piedad-Sánchez et al., 2004). Therefore, we briefly review this link with some complements. The abundance of $C_{15–19}$ *n*-alkanes can be an indicator of algal organic matter, whereas the abundance of long-chain *n*-alkanes (>C_{22}) is an indicator of the wax of higher plants (Tissot and Welte, 1984) or of spores (Allan and Douglas, 1977). The Donbas coals are vitrinite-rich (mean: 81%). Consequently, the abundance of $C_{15–19}$ *n*-alkanes should be low and a maximum should be found in $C_{20–24}$ *n*-alkanes (Allan and Douglas, 1977). However, the predominance of $C_{15–19}$ *n*-alkanes can also reflect bacterial biomass input (Peters and Moldowan, 1993). Abundance of different *n*-alkanes is variable in Donbas clastics and limestones because higher plants and algae are present together.

From our results, oxic conditions are implied for all Donbas coals and deltaic siltstones, and oxygen-depleted conditions for limestones and claystones considering that pristane and phytane are phytol diagenesis products. Pr/*n*-C_{17} ratios >1 are characteristic for inland peat-swamp environments and those < 0.5 for open-water conditions (sea and large lake, Lijmbach, 1975). If the ratio ranges from 0.5 to 1, a transitional environment between continent and sea (Volkman and Maxwell, 1986) can be expected. Based on these ratios, Donbas coals were deposited

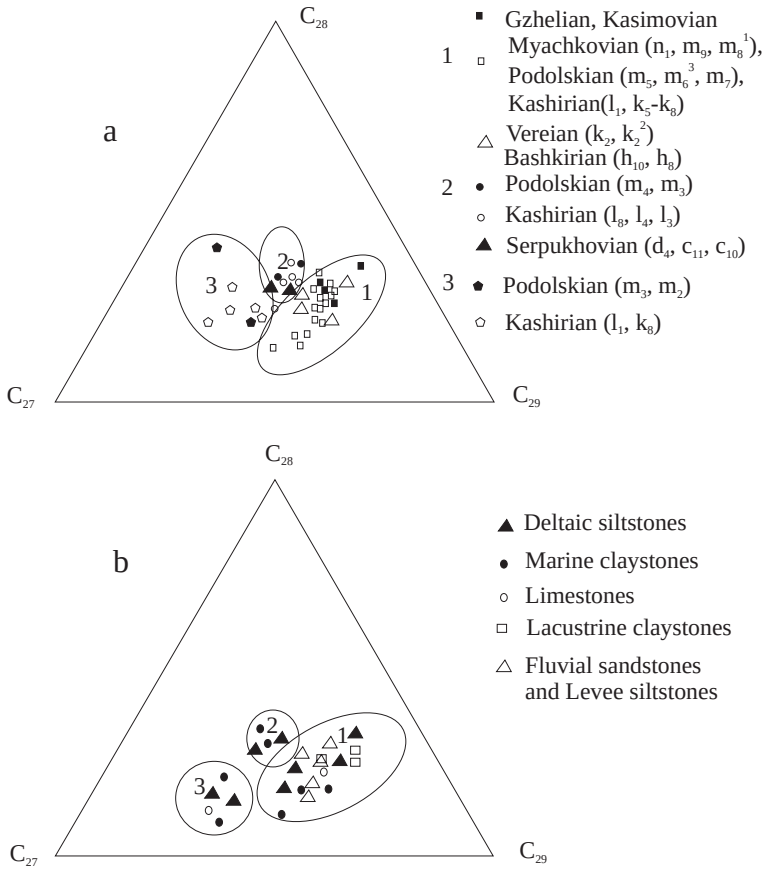

Fig. 8. % C_{27}, C_{28} and C_{29} steranes distributions for Serpukhovian to Gzhelian coals (a) and limestones and clastic rocks (b).

in a continental swamp, limestones in open-water and claystones in open-water or transitional environments. An agreement is observed between these conclusions and the sedimentology. But, because the Pr/Ph ratio is strongly influenced by maturity (Fig. 5f; Radke et al., 1980) and the amount and nature of precursors (Koopmans et al., 1999; Höld et al., 2001), it must be used with caution for the estimation of the oxic state of the depositional environment.

According to Philp (1994) diterpanes are representative in the following groups of Carboniferous plants:

- Pimaranes (2+4): pre-gymnosperms (cordaites), pteridophytes, bryophytes;
- *ent*-Beyerane (3): pre-gymnosperms;
- Kaurane (6): pre-gymnosperms, pteridophytes, bryophytes;
- Phyllocladanes (5+7): pre-gymnosperms.

The R_{dit} ratio (Section 4.4.3) described by Fleck (2001) allows determination of the relative importance of pre-gymnosperms (dominant when $R_{dit}<1$) versus pteridophytes (dominant when $R_{dit}>1$) among the peat forming vegetation. This ratio is also a measure of the comparative height of the water table in the swamp that determines the type of vegetation (low: $R_{dit}<1$; medium to high: $R_{dit}>1$). For the clastics and limestones, this ratio will be an indicator of plants that were eroded, transported and deposited during the sedimentation.

The group 1 samples are characterized by high contents in Phyllocladane and *ent*-Beyerane representative of pre-gymnosperms during the Carboniferous. The R_{dit} ratio is < 1 and indicates a low water table.

The group 2 samples are high in *iso*-Pimarane and diterpanes common to pteridophytes, pre-gymnosperms, and bryophytes. High R_{dit} ratios suggest a high water table.

The group 3 exhibits high Kaurane contents and diterpanes common to the same plants as in group 2, but with *ent*-Beyerane and Phyllocladanes known only in pre-gymnosperms. Lower R_{dit} ratios indicate a medium height or seasonally variable water table.

Huang and Meinschein (1978, 1979) plotted the relative proportions of C_{27}–C_{28}–C_{29} steranes on a ternary diagram. A decrease of C_{29} and an increase of C_{27} is observed from group 1 to group 3 for coals (Fig. 8a) and limestones and clastic rocks (Fig. 8b). High values of C_{27} steranes are found in marine limestones and claystones, deltaic siltstones and rare coals and low values in most of coals, limestones and clastic rocks.

Therefore, two possibilities can be proposed to explain the differences in the relative abundance of C_{27} and C_{29} steranes for coals: (1) C_{29} steranes are mainly derived from C_{29}-sterols from the tissues of higher plants. According to this interpretation, group 1 represents the highest input from woody plants. The C_{27} and C_{28} steranes may be derived from algal material as in lacustrine environments. Thus, the group 3 samples represent a high input of algae and a swamp with a high water table. However, alginite is a rare maceral in these coals; (2) The C_{27} and C_{28} steranes may possibly be derived from the heterotrophs (protozoa, fungia, various invertebrates) decomposing wood.

And for limestones and clastic rocks, though alginite is observed in considerable amounts in some marine claystones (MC599-28), it is rare in others (MC599-3 and-24). Therefore, there is no simple relation between steranes, higher plants and algae. Volkman (1986) and Volkman et al. (1998, 1999) presented a review of sterol markers for terrigenous and marine organic matter. These authors showed that algae produced various contents of C_{27}, C_{28} and C_{29} steranes according to the species. Only $\delta^{13}C$ isotopic analyses (Grice et al., 1996, 2001) would allow to attribute steranes to higher plants, algae or bacteria and to remove this indetermination. But, Volkman (2005) wrote that the presence of a biomarker may only provide information about the existence of a biosynthetic pathway rather the presence of a particular group of organisms. C_{27} steranes are synthesized by green algae, diatoms and fungi by diverse pathways whereas C_{28} and C_{29} steranes are synthesized by higher plants. Most of cyanobacteria and eubacteria do not synthesize steranes.

Hopanes are ubiquitous constituents of sedimentary organic matter. They are derived predominantly from the degradation of the C_{35} bacteriohopane (Ourisson et al., 1979). But ferns, bryophytes, lichens and fungi contain both sterols and C_{30} hopanoids (Rohmer et al., 1992). The samples show comparable hopane patterns, characterized by a dominance of the C_{30} hopane. The abundance of hopanes above C_{31} decreases progressively with increasing carbon number. This pattern is characteristic for the presence of bacteria in the swamp (Ourisson et al., 1979) and for an oxic-type environment (Philp and Mansuy, 1997). The hopanes/steranes ratio allows estimation of the relative abundance of bacteria versus algae and terrestrial higher plants (Boreham et al., 1994; Bechtel et al., 2001). This ratio is high in our samples from coals, marine claystones and deltaic siltstones, suggesting high bacterial activity or best preservation in these environments.

Pyrene, benzo[*e*]pyrene, and benzo[*a*]pyrene are derived from combustion of land-plants (Jiang et al., 1998). In the Donbas, arboranes/fernanes were observed in Kasimovian and Gzhelian coals. They were also reported in the Stephanian and Autunian of the Saar Basin which represent equivalent stages (Vliex et al., 1994). According to these authors, these molecules are correlated with gymnosperms. However, an algal or bacterial origin is also possible (Hauke et al., 1992a,b).

5.3. Paleoclimatic changes

Two kinds of climatic changes occurred during the Permo-Carboniferous: (1) those related to the northward shift of the continents, and (2) glacio-eustatic changes depending on glaciations and deglaciations in Gondwanaland.

Paleobotanical data suggest that, in Euramerica, the first phenomenon was responsible for progressive climatic changes, from dry during the Devonian and Tournaisian, to moderate humid in the Visean and Serpukhovian (Van der Zwan, 1981; Van der Zwan et al., 1985), with tropical humidity in the Bashkirian and Moscovian (Phillips and Peppers, 1984), a transition from humid to dry in the Kasimovian (early Stephanian), and a change to a dry climate during

the Gzhelian (late Stephanian) and Permian. Palynological data from the Donbas (Fig. 9; Inosova et al., 1976) indicate the same floral and climatic changes. Herbaceous and arborescent lycopods are found in Visean to early Serpukhovian, and lycopods and ferns in the late Serpukhovian. Arborescent ferns,

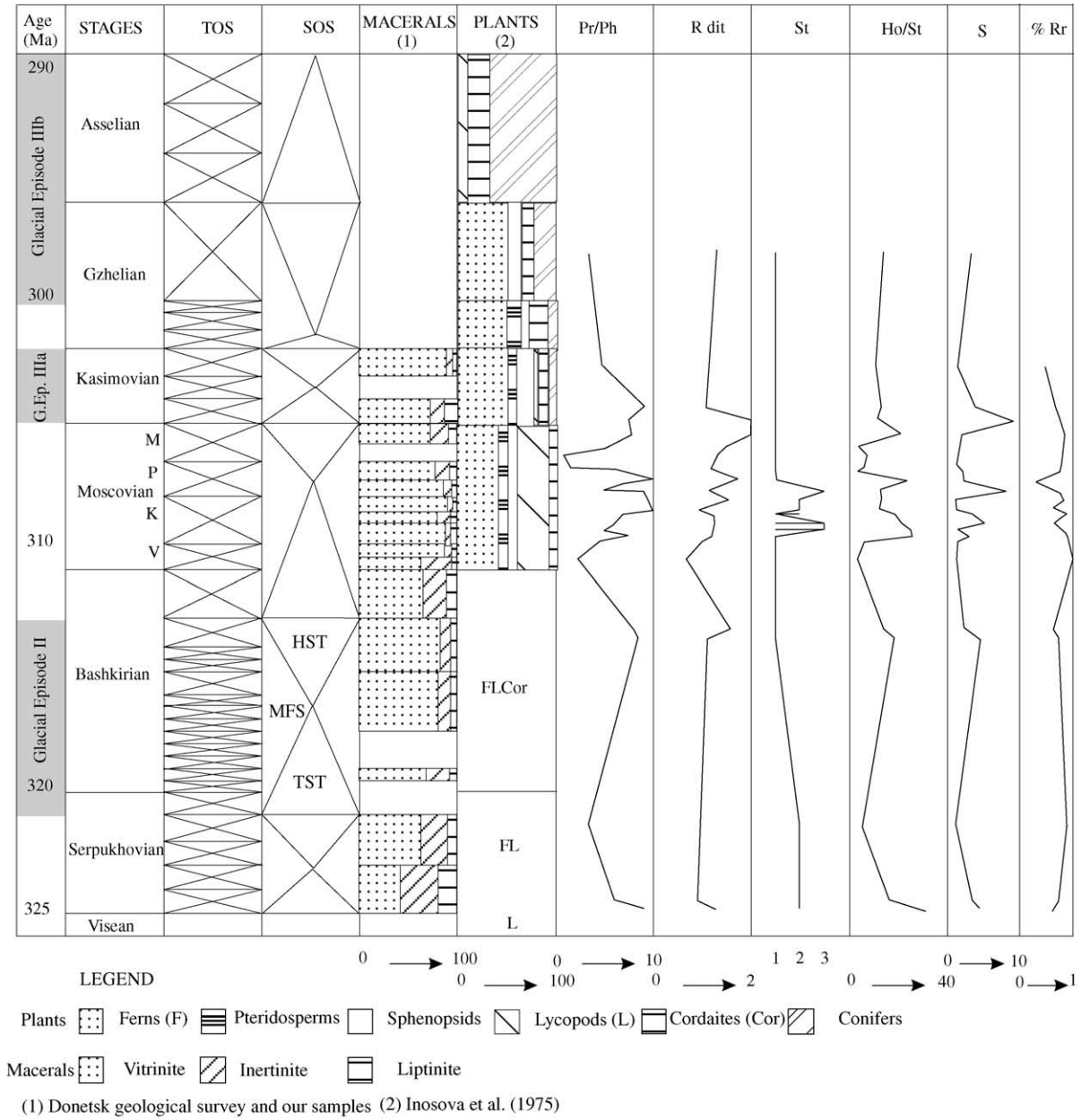

Fig. 9. Stratigraphic changes of macerals, plants and biomarkers. % C_{27}: % C_{27} steranes, FOS: fourth order sequence, Ho/St: hopanes/steranes, HST: highstand systems tract, K: Kashirian, LST: lowstand systems tract, M: Myachkovian, MFS: maximum flooding surface, P: Podolskian, Pr/Ph: pristane/phytane, *R*: Regression, R_{dit}: ratio diterpanes, % R_r: vitrinite reflectance, % S: % Sulphur, SOS: second order sequence, St: Groups of steranes, *T*: transgression, TOS: third order sequence, TST: transgressive systems tract and V: Vereian.

pteridosperms, and lycopods are indicative of an equatorial humid climate during Bashkirian and Moscovian times. An increase in gymnosperms correlates with a drier climate during Kasimovian, Gzhelian, and Permian times. The Peri–Tethys maps (Dercourt et al., 2000) place the Donbas with the equatorial zone during Moscovian and tropical zone during Artinskian (Early Permian).

The second phenomenon relates to three glacial and interglacial episodes in the Gondwanaland (Lopez-Gamundi, 1997), that correspond to global second-order sequences (SOS) between Famennian and late Permian times, when the ice cap finally disappeared:

- Glacial (Famennian–early Visean) and interglacial episode I (late Visean–Serpukhovian)
- Glacial (Bashkirian) and interglacial episode II (Moscovian)
- Glacial (Kasimovian) and interglacial episode IIIa (Gzhelian)
- Glacial (Asselian) and interglacial episode IIIb (Sakmarian)
- Glacial (Sakmarian) and interglacial episode IIIc (Artinskian–late Permian).

What was the impact of these glacial variations on coal basins located near the equator?

Cecil et al. (1985) and Cecil (1990) assessed after lithologies and paleosols a non-seasonal tropical climate with coal seams and non-calcareous siliciclastic sediments in the early to mid-middle Pennsylvanian (Bashkirian to Myachkovian) Appalachian Basin. During the remainder of the Pennsylvanian (Myachkovian to Gzhelian), the climate cycled from humid tropical with coal seams to nearly semiarid with lacustrine and pedogenic carbonates.

In our study of the Donbas, vitrinite percentages (Fig. 9) are high in lower and mid-Bashkirian, Moscovian (except lower Vereian), and upper Kasimovian coals. Liptinite contents show little stratigraphic variations. Inertinite percentages are high in coals with Serpukhovian, late Bashkirian/early Vereian, and late Myachkovian/early Kasimovian ages, indicating that burning was more important and these times were relatively dry.

The R_{dit} ratio from coals is lower in Serpukhovian, Vereian, upper Kasimovian, and Gzhelian coals, than in upper Bashkirian and Kashirian to lowermost Kasimovian coals (Figs. 9–12). This is an indication of alternating drier and wetter climates on million years time scales. Within these cycles, the Moscovian is characterized by a general trend towards higher R_{dit} ratios and wetter conditions (Figs. 9 and 11).

Phillips and Peppers (1984) postulated a maximum in climatic wetness for North American coal basins in the Desmoinesian (Myachkovian, Westphalian D). R_{dit} ratios (Fig. 10) in this level are high in Donbas coals (>1.5), in the Lorraine coal Basin (Fleck, 2001), and in the Central Asturias coal Basin (Piedad-Sánchez et al., 2004). The drier Stephanian (Late Kasimovian) and Autunian (Gzhelian) climate is supported by R_{dit} ratios close to 1 and the appearance of arborane/fernane in Donbas coals. Note that the first xerophilous plants, attesting to a dry climate, were found by Stschgolev (in Aisenverg et al., 1975) at the top of the sandstone overlying the n_3^3 coal (FOS SK2, Fig. 12). This coal is located between the n_2^3 (FOS SK1) and n_3^6 coals (FOS SK3) included in the present study. The coals n_2^2 and n_2^3 present a high R_{dit} and the coal n_3^6 a low R_{dit} ratio. This is in accordance with the first appearance of xerophilous plants in the n_3^3 coal.

The Pr/Ph ratio from coals (Figs. 9–12) is low in upper Serpukhovian, Vereian, and lower Myachkovian coals, whereas it is high in lower Serpukhovian, upper Bashkirian, Kashirian, Podolskian, upper Myachkovian, and lower Kasimovian coals. The Pr/Ph ratio suggests more oxidation of peat during the periods of wetter conditions assessed by diterpanes.

The hopanes/steranes ratio (Figs. 9–12) is low in upper Serpukhovian, Vereian, upper Podolskian, and lower Myachkovian coals; and high in lower Serpukhovian, upper Bashkirian, Kashirian, lower Podolskian, upper Myachkovian, and Kasimovian coals. Similar to group 3 steranes distribution, the high ratios are probably related to greater bacterial activity in the swamp. High values are observed in coals deposited in a peat with a high water table and a wetter climate assessed by diterpanes.

Curves representing stratigraphic changes in groups of steranes (Fig. 9) and in the percentage of C_{27} steranes (Figs. 10–12) were drawn. Coals with a group 1 steranes distribution (dominance of C_{29} ste-

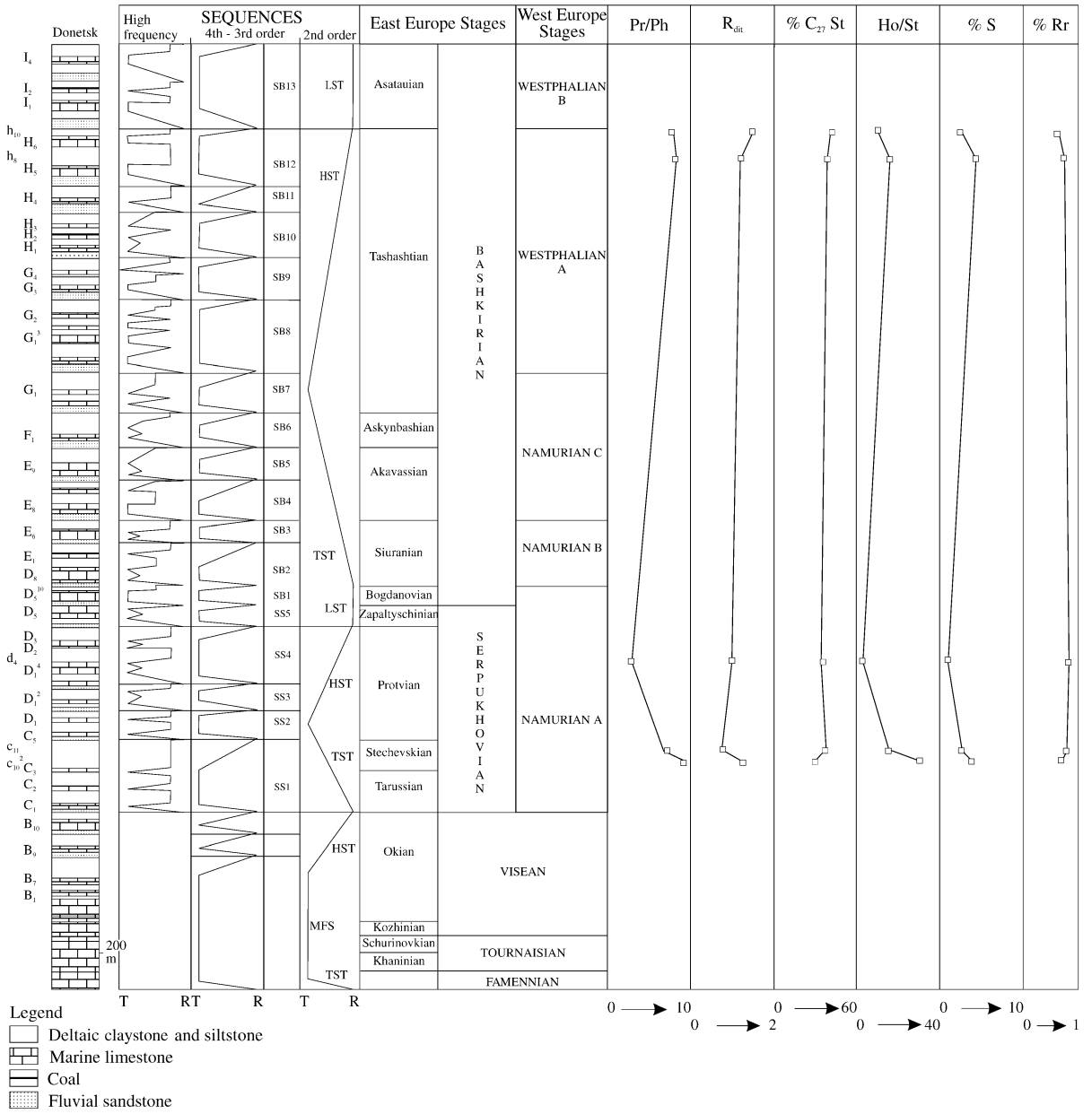

Fig. 10. Changes of biomarkers, sulphur and vitrinite reflectance of samples during Serpukhovian and Bashkirian. See legends in Fig. 9. Limestones are indicated by capitals and coal seams by lower cases.

ranes) are present in upper Bashkirian, Vereian, upper Podolskian, Myachkovian, Kasimovian, and Gzhelian horizons. Coals with group 2 (equal amounts of C_{27}, C_{28}, C_{29}) and group 3 distributions (high percentages of C_{27} and C_{28}) are present in Serpukhovian, Kashirian, and lower Podolskian levels. The presence of group 3 in Kashirian and lower Podolskian coals is probably related with a period of higher transgression and not necessarily to a period of wetter climate assessed by diterpanes.

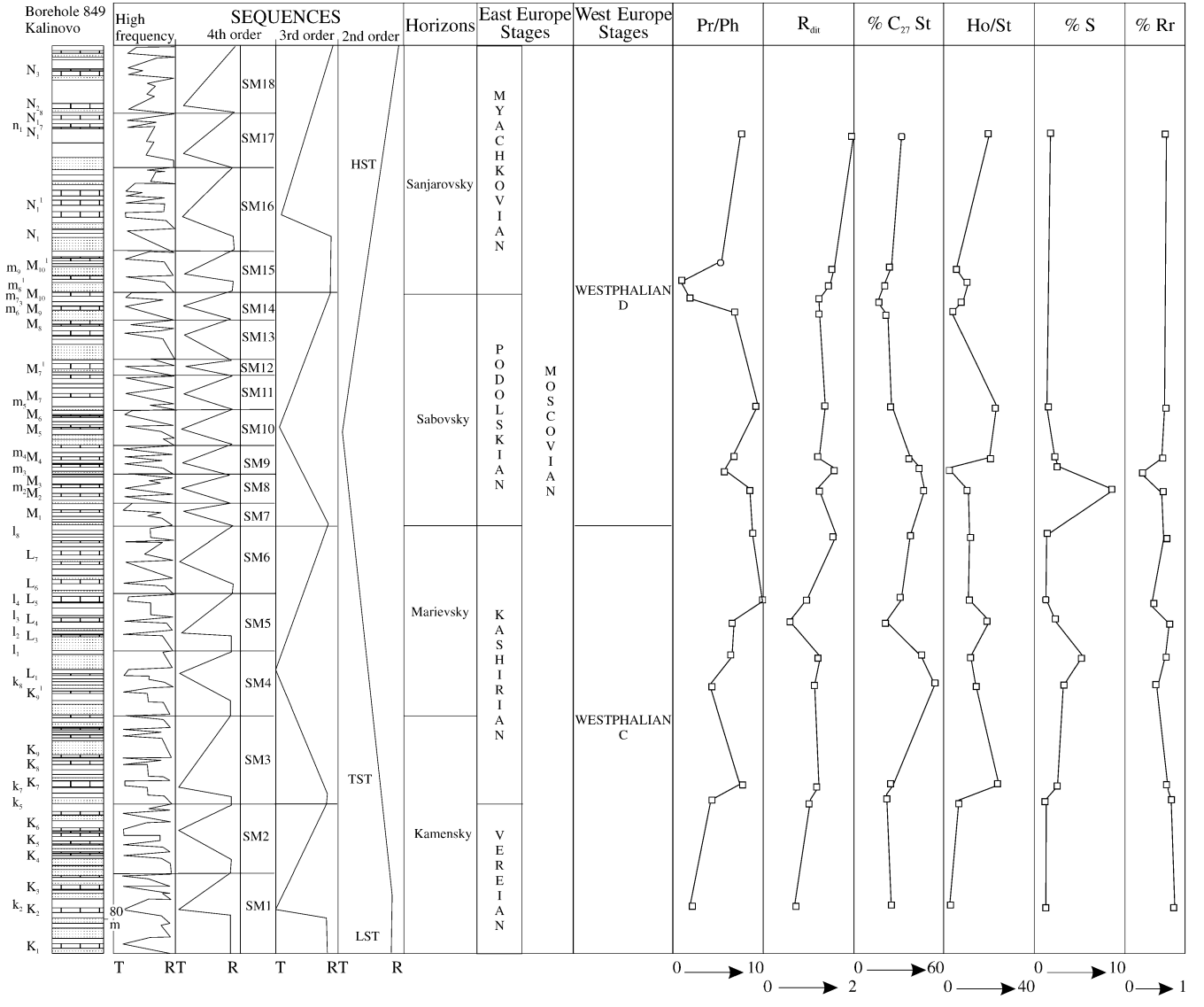

Fig. 11. Changes of biomarkers, sulphur and vitrinite reflectance of samples during Moscovian. See legends in Figs. 9 and 10.

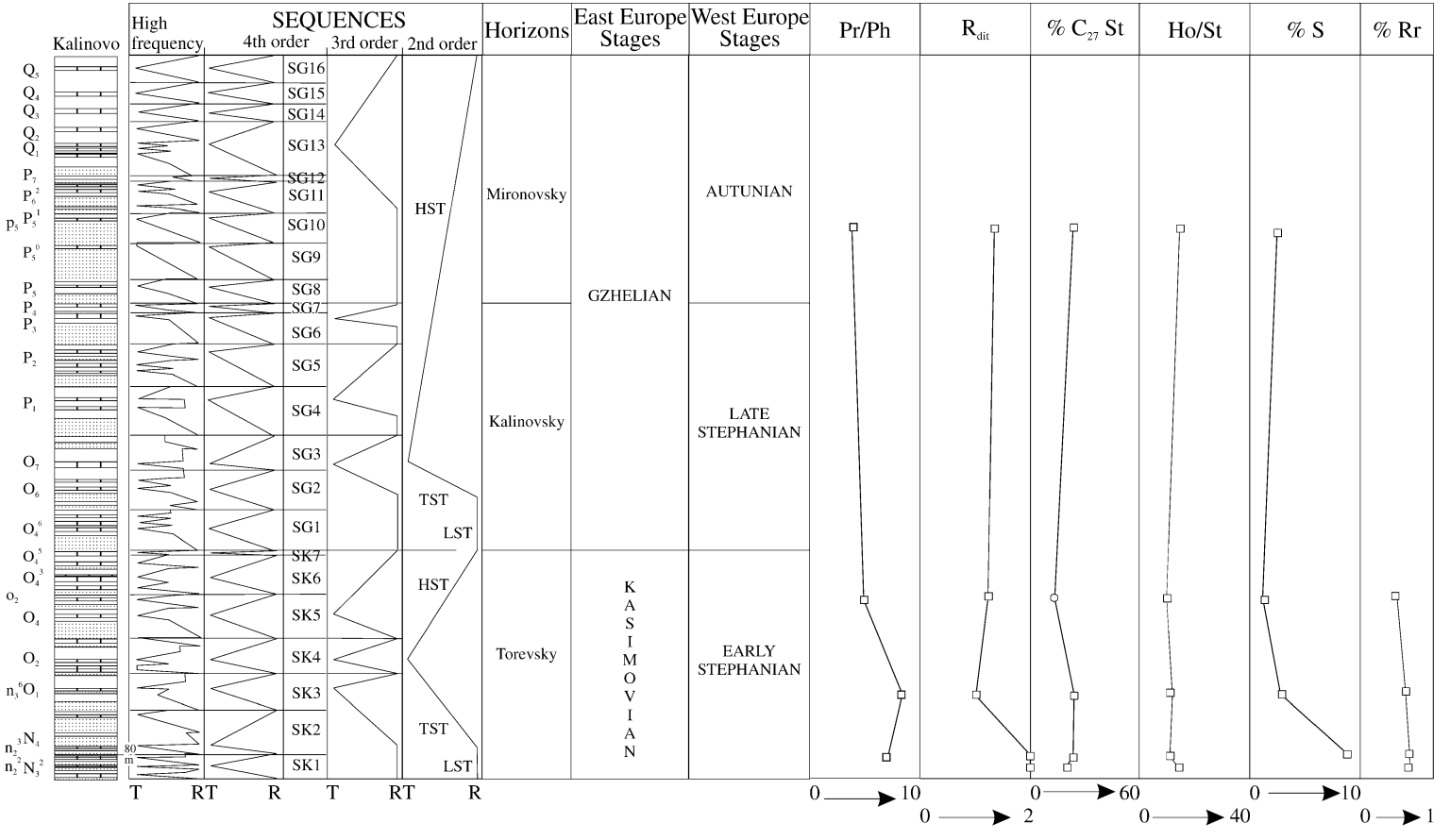

Fig. 12. Changes of biomarkers, sulphur and vitrinite reflectance of samples during Kasimovian and Gzhelian. See legends in Figs. 9 and 10.

5.4. Climatic and stratigraphic controls on coal deposition

5.4.1. High frequency sequences (HFS)

In the Donbas (Izart et al., 2002), a high frequency sequence (HFS, Fig. 13) consists of

- fluvial channel sandstone (lowstand systems tract; LST),
- paleosol, coal seam and limestone (transgressive systems tract; TST),
- marine claystone with pelagic fauna indicative for high bathymetry (maximum flooding surface; MFS),
- deltaic siltstone and sandstone (highstand systems tract; HST).

(Figs. 3, 10–13) exhibit examples of lithological columns and curves of HFS in the Donbas. Note that according to Ukrainian usage, marine bands are indicated by capital letters (e.g. K_1, Fig. 11), whereas coal seams are indicated by lower-case letters (e.g. k_2, Fig. 11). The curves of sequences of diverse orders were built by sorting the paleoenvironments between two trends, marine at the left and continental at the right to follow the retrogradation and transgression (*T*) towards the west and the progradation and regression (*R*) towards the east of the Donbas. The coal is always intercalated between underlying sandstone or paleosol, and overlying shale or limestone, and is interpreted by us as the beginning of the TST of HFS.

Coal is always observed at the boundary between continental and marine facies in all Carboniferous paralic coal basins of western Europe (North France, England and Ruhr basins, Izart and Vachard, 1994) and in the central Appalachian Basin (Chesnut, 1994),

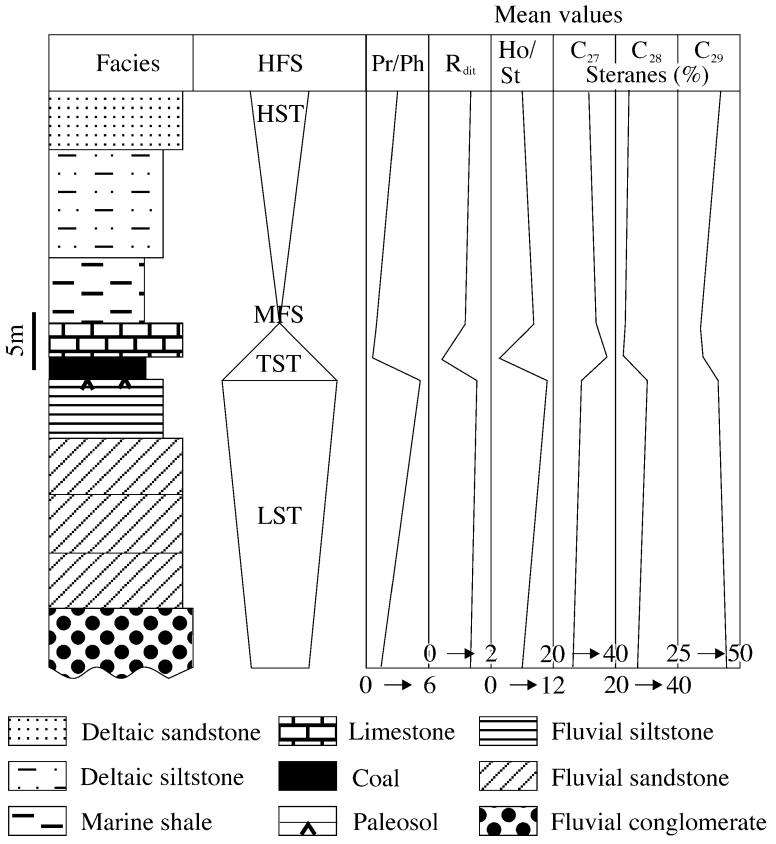

Fig. 13. High frequency sequence (HFS) of the Donbas HST: highstand systems tract, LST: lowstand systems tract, MFS: maximum flooding surface and TST: transgressive systems tract.

where peat formation was initiated by a renewed transgression.

Cecil (1990) proposed a relationship between lithology and paleoclimate and suggested a wet climate during deposition of coal and siliciclastics and a dry climate during deposition of limestone and marine shales. If this model is applied to the Donbas, the climate would be wet during the LST, early TST and the HST, and dry during the late TST and the MFS.

Cecil et al. (2003) described a Pennsylvanian cyclothem characteristic for North American coal basins, consisting of weathered paleosol, coal, marine claystone, deltaic siltstone and sandstone and fluvial channel sandstone or limestone. In contrast with our interpretation in the Donbas, these authors attributed the paleosol and the coal seam to the LST, the marine claystone to the TST, and the deltaic siltstone and fluvial sandstone (Appalachian Basin) or limestone (Illinois and Midcontinent basins) to the early and late HST of this cyclothem. Cecil et al. (2003) described the mid-Pennsylvanian climate across North America: (1) during glacial intervals, low pressure belts caused non-seasonal wet conditions in low latitude with intense weathering of paleosols and peat formation; whereas (2) during interglacial intervals, seasonal swings replaced the low-pressure belt and produced a more seasonal drier climate. Ziegler et al. (1997) also suggested that rainfall increased in equatorial latitude during glacial periods.

Miller et al. (1996) and Olszewski and Patzkowsky (2003) studied the upper Pennsylvanian to lower Permian (Gzhelian–Asselian) in the US Midcontinent and concluded that the coal is located in the upper part of HST of fifth-order sequences. For these authors, an evolution of paleosols from vertic to calcic suggests a change from a wet to an arid climate during the LST of these sequences. An arid climate persisted during the evaporitic, carbonate TST and was followed by a relatively humid coaly, siliciclastic HST. The authors used a paleoclimatic model of Miller and West (1993) to explain the observed changes: During glacial intervals, the monsoon was weak and did not bring equatorial humidity to the latitude of the Midcontinent (~10° N). During interglacial intervals, the monsoon was stronger and monsoonal rains did reach the Midcontinent. This model differs from that of Cecil et al. (2003) in a wet upper part of the HST. It also differs from the model of Perlmutter and Matthews (1989), in which the glacial event is dry because of high equatorial pressures and the interglacial event is wet because of low pressures and because the monsoon would be weak and not yet established during Carboniferous times.

5.4.2. Fourth and Third order sequences (FOS and TOS, respectively)

Diessel (1992, p. 506) discussed the sequence stratigraphic interpretation of coal seam settings. Coal seams are present in both TST and HST of FOS and TOS and exhibit different petrographic composition. In the paralic coal basins of western Europe (Izart and Vachard, 1994) and of the Donbas (Izart et al., 1996, 1998), the FOS and TOS consist of numerous HFS with sandstone, coal, and marine facies overlain by deltaic facies during the TST, and numerous HFS with sandstone, coal, and either lagoonal or lacustrine facies overlain by deltaic facies during the HST. The lithological column compared with FOS and TOS columns (Figs. 10–12) exhibit the place of coals during TST and HST in the Donbas.

The cyclothem described by Cecil et al. (2003) in the Illinois and the Midcontinent basins was shown previously by Heckel (1994, his Figs. 1 and 8). It corresponds to the major transgressive cycle Verdigris during Desmoinesian and is followed by three minor transgressive cycles. These four cycles corresponding to HFS constitute a FOS with a TST (major cycle) with coal and limestone at the lower part and a HST (three minor cycles) with coal and marine claystone in the upper part. In this FOS, coal seams are also present in TST and HST as in all paralic basins. For Miller et al. (1996) and Olszewski and Patzkowsky (2003), the FOS and TOS of the US Midcontinent include HFS with limestone, claystone and coal during the TST and limestone, claystone, sandstone and coal during the HST. The relation between climate and eustacy for FOS and TOS in the Midcontinent may be offset (Miller et al., 1996), with wet climate during HST and LST and dry climate during TST and MFS.

5.4.3. Second order sequences (SOS)

The second order sequences (SOS) in the Donbas correspond to the Serpukhovian, Bashkirian, Moscovian, Kasimovian, and Gzhelian stages (Fig. 9, Izart et al., 2003). The Moscovian includes a TST during the Vereian and Kashirian, a MFS during the Podolskian

(M_5 limestone) and a HST during the Myachkovian (Fig. 11, Izart et al., 1996). A peak in climatic wetness during Desmoinesian (Myachkovian, Westphalian D) times is reported for coal basins in the USA (Phillips and Pepper, 1984), in Central Asturias (Piedad-Sánchez et al., 2004), and for the Donbas (this paper). This period corresponds to the HST of the Moscovian SOS. The (Figs. 10–12) exhibit the increase of marine limestones during the MFS (Podolskian) and the place of coals during all system tracts of SOS in the Donbas. However, the coal seams appeared during the Serpukhovian SOS, increased during the Bashkirian SOS, reached a maximum during the Moscovian SOS, then the coal decreased during the Kasimovian SOS and finally disappeared during the Gzhelian SOS as in the western Europe (Izart et al., 2003).

5.5. Relationship between maceral and biomarker data and glacio-eustatic changes

The changes of biomarkers in Fig. 14 don't represent all variations of lithology and sequence (Fig. 3) because the sampling is incomplete. Only a statistical treatment of data (Figs. 13 and 15, Table 5) allows to check these fluctuations for HFS. A statistical study was also carried out using maceral and biomarker for FOS, TOS, and SOS (Fig. 16, Table 5) to identify differences related to glacio-eustatic changes. Biomarkers exhibit major differences between sandstones, claystones and coals (see Fleck (2001) for the Lorraine Basin (France) and our data for the Donbas). Thus, calculating mean values using data from different lithologies is agreed useless. Therefore, our statistical study is based on clastics and coals for HFS (Figs. 13 and 15, Table 5), but is restricted to coals for FOS, TOS and SOS (Fig. 16, Table 5). Consequently, our paleoclimatic interpretations concern the time of coal and clastic deposition for HFS, but only the time of coal deposition for other sequences.

The selection of samples for biomarker studies is discussed in Section 5.1. To test potential differences, the statistical study was repeated with a limited sample set including fifty coal samples with a VR < 0.8% (groups 1 and 2 according to Fig. 6a), three limestones and thirty-three clastic samples, which are compared to thirteen coeval coal samples.

The mean values for all Carboniferous coals and for a Myachkovian to Kasimovian subset are similar. Only the R_{dit} value is significantly higher for the latter (1.76, $n=13$) than for all coals (1.16, $n=50$). This is because the Myachkovian to Kasimovian climate was wetter than the lower Moscovian one.

The observed trends for different systems tracts for sequences of different order are generally the same, but slight differences occur in absolute values. The TST of SOS, MFS of TOS and HST of FOS with a great number of samples (22–28) or parameters with a low standard deviation σ (V/V+I, C_{27}, C_{28} and C_{29} steranes) are statistically more significant than systems tracts with a low sample number or with a high σ (S, Pr/Ph and H/S). Note that R_{dit} (Table 5) presents a high σ in LST of SOS and a low σ for other system tracts of SOS and other sequences.

The vitrinite/(vitrinite+inertinite) (V/(V+I)) ratio is highest in coals formed during the TST and the MFS of different sequences, and is relatively low in coals deposited during the LST of SOS. Although pyrofusinite may be blown or washed into the depositional environment, a low V/(V+I) ratio is generally considered to indicate oxidation and relatively dry peat forming conditions. Therefore, relatively low ratios during the LST of SOS suggest a relative aridity. But, two populations of samples, one rich in vitrinite and the other in inertinite are demonstrated by high values of σ existed certainly during LST. Strehlau (1990) described also in the Ruhr Basin an increase of inertinite linked with burning in the upper part of the Bashkirian sequence and in the lower part of the Moscovian sequence.

Liptinite percentages (Table 5) show a maximum during the HST of FOS and TOS. Regarding SOS, liptinite percentages are low during the LST and reach a maximum during early TST and HST. Liptinite percentages, similar to vitrinite, are linked with the increase of organic productivity or preservation in the swamp during wetter periods.

The R_{dit} ratio of coals (Fleck, 2001) allows estimation of the level of the water table in the swamp (low: $R_{dit}<1$; medium to high: $R_{dit}>1$) and the paleoclimate. The variable R_{dit} of coals suggest for the HFS a coincidence or a delay between the beginning of transgression and dry climate when R_{dit} is low or high, respectively. For HFS (Figs. 13–15, Table 5), the R_{dit} exhibits intermediate values during LST (mean: 1.22), high to intermediate values during early TST1 (1.5 for

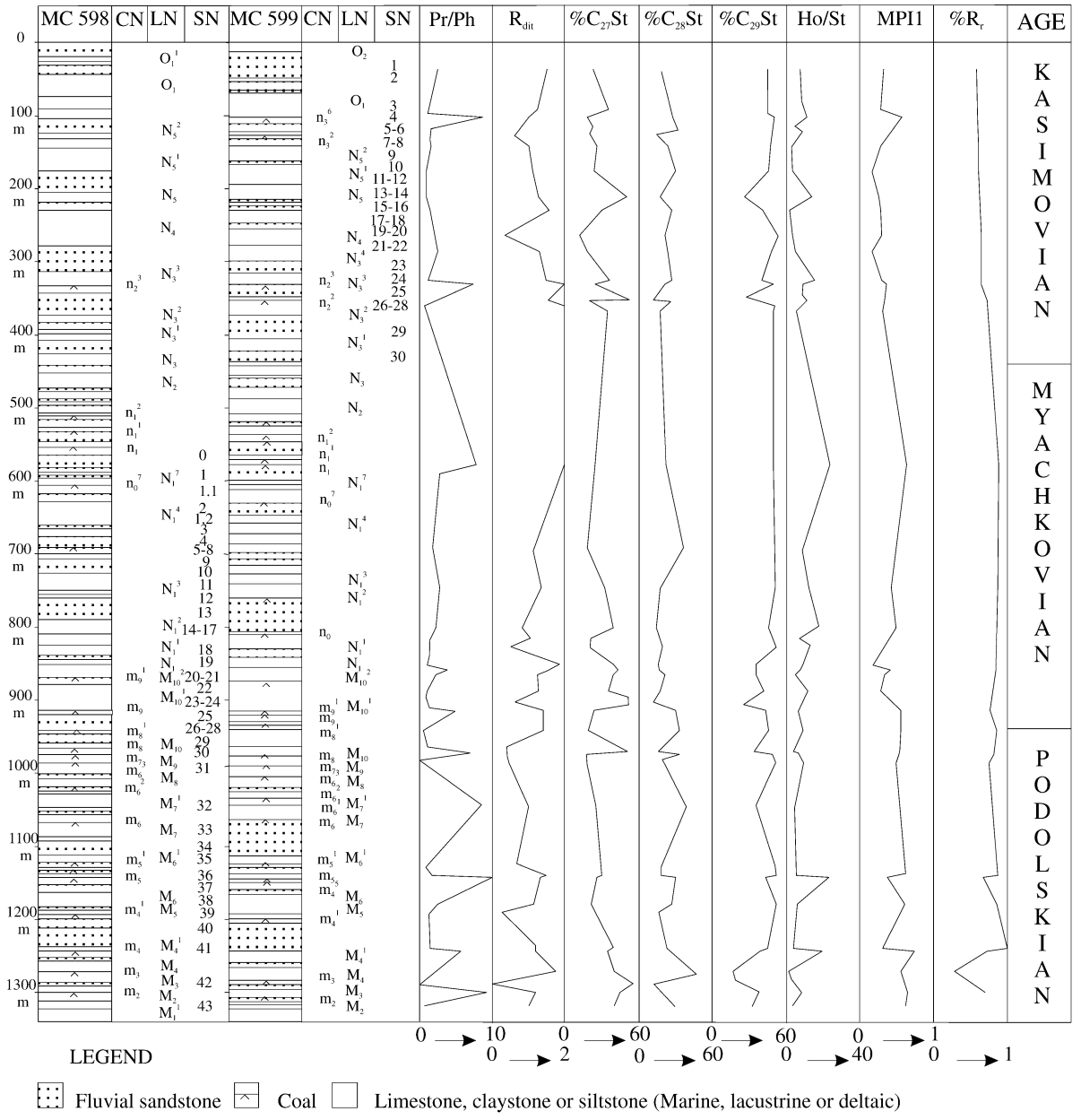

Fig. 14. Changes of biomarkers in the MC598 and MC599 boreholes CN: coal number, LN: marine band number and SN: sample number.

the interval Podolskian–Kasimovian, but 1.16 for all the Carboniferous), low values during late TST2 (0.56), during MFS (1.1) and HST (1.1). The R_{dit} suggests for HFS an intermediate climate during LST (fluvial sandstone), a wet to dry climate during early TST1 (coal) and a dry climate during late TST2 (limestone), MFS (marine claystone) and HST (deltaic siltstone). The R_{dit} of coals decreases from LST

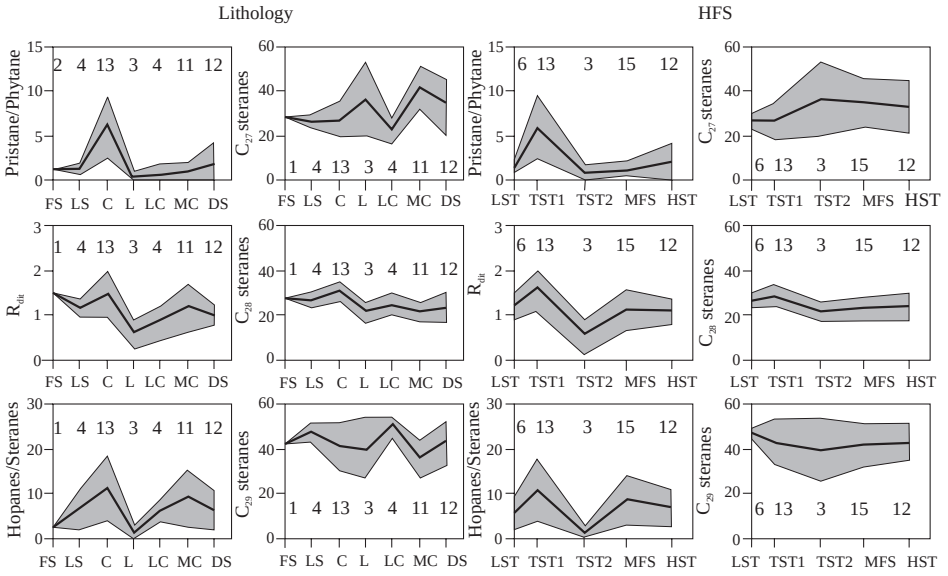

Fig. 15. Changes of biomarkers for different lithologies and high frequency sequences (HFS) for the Podolskian, Myachkovian and Lower Kasimovian. HST: highstand systems tract, LST: lowstand systems tract, MFS: maximum flooding surface, TST1: early transgressive systems tract (coal) and TST2: late transgressive systems tract (limestone). FS: fluvial sandstone, LS: levee siltstone, C: coal, LC: lacustrine claystone, MC: marine claystone and DS: deltaic siltstone. The numbers correspond to the number of samples in each systems tract. The curve represents the mean of data and the shaded zone the mean + or − the standard deviation. Minimum and maximum are provided in the Table 5.

(1.36) to early TST (1.16), then increases to HST(1.35) for FOS, TOS, and SOS. The LST of TOS and SOS presents two populations of samples as demonstrated by high values of σ: coals from Vereian with low values of R_{dit} and coals from lower Kasimovian with high values. The R_{dit} suggests for SOS a relatively dry climate for LST of Vereian, and wet climate for LST of Kasimovian, an intermediate to wet climate for early TST and MFS and a relatively wet climate for HST. This trend and consequently this paleoclimatic change are observed also for TOS and FOS.

Pr/Ph ratio show high values for HFS (Figs. 13–15) during early TST1 (mean: 5.75), intermediate during HST (2), and low values during late TST2 (0.64), MFS (1.29) and LST(1.3). For FOS and TOS, Pr/Ph ratio from coals exhibit high values during the early TST and the HST, intermediate during MFS, but relatively low values during the LST. For SOS, this ratio show low values during the LST (mean: 3.4) and generally high values during the early TST (7.55), MFS, and HST. But, high σ values show that the variability is important for all system tracts and sequences. If we compared with the paleoclimates deduced from diterpanes, the highest oxidation corresponds to the wettest period and conversely.

The hopanes/steranes ratio exhibit low values for HFS (Figs. 13–15) during late TST2 (mean: 1.87), intermediate during LST (6.22), HST (6.67) and MFS (8.32), and high (11.15) during early TST1. This ratio is low for SOS in the LST (5), intermediate in MFS (11), and high in early TST (16) and HST (13). The same trend is observed for sequences with different order. If we compared with diterpanes and Pr/Ph, the hopanes/steranes ratio shows that bacteria were more active in the swamp during periods with a wettest climate and high oxidation.

The maximum of C_{27} steranes (37%) and the minimum of C_{29} steranes (41%) are observed for HFS (Figs. 13–15) in rocks deposited in the late TST2 and the MFS, whereas the C_{28} steranes present only a small change. Coals deposited near the MFS contain the highest amount of C_{27} steranes linked to algae and the lowest amount of C_{29} steranes derived from wood of terrestrial higher plants. The abundance of C_{27} steranes increases for SOS from the LST (24%) to the TST (34%) or MFS (35%) and decreases in the

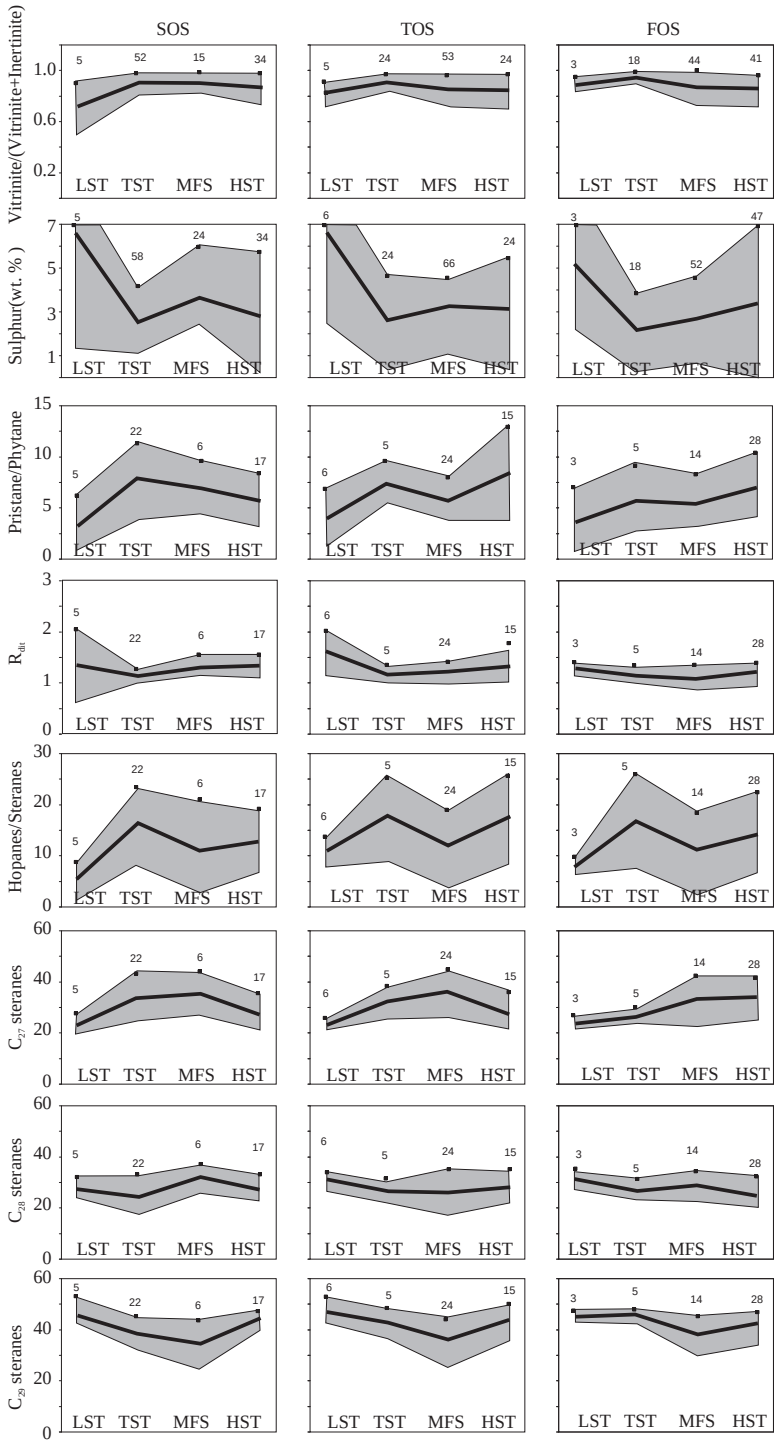

Fig. 16. Changes of macerals, sulphur and biomarkers during different systems tracts in the second order sequences (SOS), third order sequences (TOS), and fourth order sequences (FOS) from Serpukhovian to Gzhelian. See legends in Fig. 15.

HST (27%). The same trend is observed for diverse sequences. The percentage of C_{28} steranes is about the same in all systems tracts and sequences, but reaches a maximum in the MFS or LST. C_{29} steranes are high for SOS in the LST (47%), and the HST (44%), intermediate in TST (40%), and low in MFS (34%). The same relationship between the steranes and eustacy is observed for diverse sequences. Although part of the C_{28} steranes may be produced by heterotrophic organisms (protozoa, fungi, invertebrates), this interpretation fits well with a high-water table prevailing during the MFS.

The results for HFS support the paleoclimatic model of Cecil et al. (2003): an intermediate paleoclimate during LST (sandstone and levee siltstone), a wet climate during early TST (paleosol and coal), and a dry climate during late TST (limestone), MFS (claystone), and HST (deltaic siltstone). The results for SOS, TOS and FOS during the coal deposition involve a relatively dry or wet paleoclimate during LST, intermediate or wet during the TST and the MFS, and relatively wet during the HST. Some parameters (e.g. macerals, diterpanes, pristane/phytane, and hopanes/steranes) are linked mainly with paleoclimate and others (e.g. steranes) with the transgression of the sea. But offset and lag times can exist between paleoclimate and eustacy for sequences of different order.

6. Conclusions

A relationship between the distribution of macerals, biomarkers, and paleoenvironment was demonstrated for the Donbas. Because of maturity effects, the Pr/Ph ratio cannot be applied as a measure for eH conditions in our study. The diterpanes can be used to assess the input of diverse plant groups and the height of the water table in the swamp; the hopanes are indicative for bacterial activity in the peat. Steranes allow to assess the input of wood- and algal-derived kerogen in the peat. The aromatics exhibit PAHs linked with the combustion of wood. The occurrence of arborane/fernane is linked with the appearance of gymnosperms and is restricted to Kasimovian and Gzhelian coals.

For the relationship between the distribution of macerals, biomarkers, and paleoclimatic and eustatic changes, two kind of climatic changes must be distinguished during the Permo-Carboniferous in the Donbas: (1) climatic changes due to the northward shift of the continents as demonstrated by Carboniferous plants of an equatorial climate that evolved to plants of a dry climate during the Permian, and (2) glacio-eustatic changes depending of the frost and melt of the ice cap in the Gondwanaland.

A tropical climate prevailed in the Donbas from the Serpukhovian to the Kasimovian. Nevertheless, periods with relatively dry and wet conditions can be distinguished based on maceral (vitrinite, inertinite) and biomarker (diterpanes, hopanes) data. Relatively dry conditions are observed during Serpukhovian and Vereian times; whereas wetter climates with a maximum of coal deposition occurred during the Bashkirian, most of the Moscovian, and the earliest Kasimovian. No economic coal seams are hosted in upper Kasimovian and Gzhelian deposits, a result of a change to a dry climate.

For the second order, third order and fourth order sequences of the Donbas, coal deposition during lowstand systems tracts is characterized by relatively dry or wet conditions. An intermediate climate occurred during the transgressive systems tract and maximum flooding, and the wettest conditions during the highstand systems tract. The results for HFS support the paleoclimatic model of Cecil et al. (2003) and the results for SOS, TOS and FOS during coal deposition show some differences with this model. Maceral and biomarker data suggest that coal deposition during high frequency sequences could be produced under wet or relative dry climate, which indicates the coincidence or delay between eustacy and paleoclimate.

Acknowledgments

The French and Ukrainian Foreign Offices are gratefully acknowledged for the financing of a part of this work by the French–Ukrainian co-operation Dnipro project. R.F.S gratefully acknowledges financial support by the Austrian Science Foundation (FWF project 14895). A.S. was supported by the Austrian Exchange Service (ÖAD). Finally, we thank J.C. Hower and reviewers for the constructive reviews of the manuscript.

References

Aisenverg, D.E., Lagutina, V.V., Levenstein, M.L., Popov, V.S., 1975. Field excursion guide book for the Donets Basin. C.R.. 8th International Congress of Carboniferous Stratigraphy and Geology, Moscow. 360 pp.

Allan, J., Douglas, A.G., 1977. Variations in the content and distribution of *n*-alkanes in a series of carboniferous vitrinites and sporinites of bituminous rank. Geochimica et Cosmochimica Acta 41, 1223–1230.

Alpern, B., Lemos de Sousa, M.J., 2002. Documented international enquiry on solid sedimentary fossil fuels; coal: definitions, classifications, reserves-resources, and energy potential. International Journal of Coal Geology 50, 3–41.

Bechtel, A., Gruber, W., Sachsenhofer, R.F., Gratzer, R., Püttmann, W., 2001. Organic geochemical and stable carbon isotopic investigation of coals formed in low-lying and raised mires within the Eastern Alps (Austria). Organic Geochemistry 32, 1289–1310.

Belokon, V.G., 1971. Geological history of evolution of the Donbas (in Russian). Geology and Prospecting of Coal Deposits. Nedra, Moscow, pp. 3–15.

Boreham, C.J., Summons, R.E., Roksandic, Z., Dowling, L.M., Hutton, A.C., 1994. Chemical, molecular and isotopic differentiation of organic facies in the Tertiary lacustrine Duaringa oil shale deposit, Queensland, Australia. Organic Geochemistry 21, 685–712.

Cecil, C.B., 1990. Paleoclimate controls on stratigraphic repetition of chemical and siliciclastic rocks. Geology 18, 533–536.

Cecil, C.B., Stanton, R.W., Neuzil, S.G., Dulong, F.T., Ruppert, L.F., Pierce, B.S., 1985. Paleoclimate controls on Late Paleozoic sedimentation and peat formation in the Central Appalachian Basin (U.S.A.). International Journal of Coal Geology 5, 195–230.

Cecil, C.B., Dulong, F.T., West, R.R., Stamm, R., Wardlaw, B.A., Edgar, N.T., 2003. Climate controls on the stratigraphy of a Middle Pennsylvanian cyclothem in North America. In: Cecil, C.B., Edgar, N.T. (Eds.), Climate Controls on Stratigraphy, SEPM Special Publication, vol. 77, pp. 151–180.

Chesnut Jr., D.R., 1994. Eustatic and tectonic control of deposition of the Lower and Middle Pennsylvanian strata of the Central Appalachian Basin. In: Dennison, J.M., Ettensohn, F.R. (Eds.), Tectonic and Eustatic Controls on Sedimentary Cycles, SEPM Concepts in Sedimentology and Paleontology, vol. 4, pp. 51–64.

Dercourt, J., Gaetani, M., Vrielynck, B., Barrier, E., Biju-Duval, B., Brunet, M.F., Cadet, J.P., Crasquin, S., Sandulescu, M., 2000. Atlas Peri–Tethys, Palaeogeographical maps. CCGM/CGMW, Paris, 24 maps and explanatory notes: I-XX; 1-269.

Deutsches Institut für Normung, 1978. Feste Brennstoffe; Bestimmung des Wassergehaltes. DIN 51718.

Deutsches Institut für Normung, 1980. Feste Brennstoffe; Bestimmung des Aschegehaltes. DIN 51719.

Didyk, B.M., Simoneit, B.R.T., Brassell, S.C., Eglinton, G., 1978. Organic geochemical indicators of paleoenvironmental conditions of sedimentation. Nature 272, 216–222.

Diessel, C.F.K., 1992. Coal-Bearing Depositional Systems. Springer, Berlin. 721 pp.

Eglinton, T.I., Douglas, A.G., Rowland, S.J., 1988. Release of aliphatic, aromatic and sulphur compounds from Kimmeridge kerogen by hydrous pyrolysis: A quantitative study. In: Mattavelli, L., Novelli, L. (Eds.), Advances in Organic Geochemistry 1987: Part II. Analytical geochemistry, Organic Geochemistry, vol. 13, pp. 655–663.

Einor, O.L., 1996. The former USSR. In: Wagner, R.H. (Ed.), The Carboniferous of the Word III, The Former USSR, %Mongolia, Middle East Platform, Afghanistan, and Iran, IUGS Publ., vol. 33. Instituto Geologico y Minero de Espana, Madrid, pp. 13–407.

Espitalié, J., Laporte, J.L., Madec, M., Marquis, F., Leplat, P.M., Paulet, J., Boutefeu, A.P., 1977. Méthode rapide de charactérisation des roches mères de leur potentiel pétrolier et de leur degré d'evolution. Revue de l'Institut Francais du Pétrole 32, 23–43.

Fleck, S., 2001. Corrélation entre géochimie organique, sédimentologie et stratigraphie séquentielle pour la caractérisation des paléoenvironnements de dépôt. PH. D. Thesis, université Henri Poincaré, Nancy 1. 387 pp.

Fleck, S., Michels, R., Izart, A., Elie, M., Landais, P., 2001. Palaeoenvironmental assessment of Westphalian fluvio-lacustrine deposits of Lorraine (France) using a combination of organic geochemistry and sedimentology. International Journal of Coal Geology 48, 65–88.

Grice, K., Schaeffer, P., Schwark, L., Maxwell, J.R., 1996. Molecular indicators of paleoenvironmental conditions in an immature Permian shale (Kupferschiefer, Lower Rhine Basin, northwest Germany) from free and S-bound lipids. Organic Geochemistry 25, 131–147.

Grice, K., Audino, M., Boreham, C.J., Alexander, R., Kagi, R.I., 2001. Distribution and stable carbon isotopic compositions of biomarkers in torbanites from different palaeogeographical locations. Organic Geochemistry 32, 1195–1210.

Han, Z., Yang, Q., Pang, Z., 2001. Artificial maturation study of a humic coal and a torbanite. International Journal of Coal Geology 46, 133–143.

Hauke, V., Graff, R., Wehrung, P., Trendel, J.M., Albrecht, P., Schwark, L., Keely, B.J., Peakman, T.M., 1992. Novel triterpene-derived hydrocarbons of Arborane/Fernane series in sediments: Part I. Tetrahedron 48 (19), 3915–3924.

Hauke, V., Graf, R., Wehrung, P., Trendel, J.M., Albrecht, P., Riva, A., Hopfgartner, G., Gülaçar, F.O., Buchs, A., Eakin, P.A., 1992. Novel triterpene-derived hydrocarbons of the arborane/fernane series in sediments: Part II. Geochemica et Cosmochimica Acta 56, 3595–3602.

Heckel, P.H., 1994. Evaluation of evidence for glacio-eustatic control over marine Pennsylvanian cyclothems in North America and consideration of possible tectonic effects. In: Dennison, J.M., Ettensohn, F.R. (Eds.), Tectonic and Eustatic Controls on Sedimentary Cycles, SEPM Concepts in Sedimentology and Paleontology, vol. 4, pp. 65–87.

Hess, J.C., Lippolt, H.J., 1986. $^{40}Ar/^{39}Ar$ ages of tonstein and tuff sanidines: New calibration points for the improvement of the Upper Carboniferous time scale. Isotopic Geosciences 59, 143–154.

Höld, I.M., Schouten, S., van der Gaast, S.J., Sinninghe Damsté, J.S., 2001. Origin of prist-1-ene and prist-2-ene in kerogen pyrolysates. Chemical Geology 172, 201–212.

Huang, W.Y., Meinschein, W.G., 1976. Sterols as source indicators of organic materials in sediments. Geochimica et Cosmochimica Acta 40, 323–330.

Huang, W.Y., Meinschein, W.G., 1979. Sterols as ecological indicators. Geochimica et Cosmochimica Acta 43, 739–745.

Inosova, K.I., Kruzina, A.H., Schvatsman, E.G., 1976. Atlas of Microspores and Pollens from the Upper Carboniferous and Lower Permian of the Donets Basin (in Russian). Nedra, Moscow. 176 pp.

Izart, A., Vachard, D., 1994. Tectonic subsidence, eustacy and control of the sequences in the Namurian and Westphalian basins of the western Europe, CIS and USA. Bulletin de la Société géologique de France 165, 499–514.

Izart, A., Briand, C., Vaslet, D., Vachard, D., Coquel, R., Maslo, A., 1996. Stratigraphy and sequence stratigraphy of the Moscovian in the Donets basin. Tectonophysics 268, 189–209.

Izart, A., Briand, C., Vaslet, D., Vachard, D., Broutin, J., Coquel, R., Maslo, A., Maslo, N., Kotzinskaya, R., 1998. Stratigraphy and sequence stratigraphy of the Upper Carboniferous and Lower Permian in the Donets Basin. In: Crasquin-Soleau, S., Barrier, É. (Eds.), Stratigraphy and Evolution of Peri–Tethyian Platforms, Peri–Tethys Memoir 3, vol. 177. Mémoires du Muséum National d'Histoire Naturelle, Paris, pp. 9–33.

Izart, A., Vachard, D., Vaslet, D., Maslo, A., 2002. Sedimentology of the Upper Carboniferous and Lower Permian in the Dniepr and Donets basins. In: Hills, L.V., Henderson, C.M., Bamber, E.W. (Eds.), Carboniferous and Permian of the World, Canadian Society of Petroleum Geologists, Memoir, vol. 19, pp. 120–143.

Izart, A., Stephenson, R., Vai, G.B., Vachard, D., Le Nindre, Y., Vaslet, D., Fauvel, P.-J., Süss, P., Kossovaya, O., Zhongquiang, C., Maslo, A., Stovba, S., 2003. Sequence stratigraphy and correlation of late Carboniferous and Permian in the CIS, Europe, Tethyan area, North Africa, Arabia, China, Gondwanaland and the USA. Palaeogeography, Palaeoclimatology, Palaeoecology 196, 59–84.

Jiang, C., Alexander, R., Kagi, R.I., Murray, A.P., 1998. Polycyclic aromatic hydrocarbons in ancient sediments and their relationship to paleoclimate. Organic Geochemistry 29, 1721–1735.

Killops, S.D., Funnell, R.H., Suggate, R.P., Sykes, R., Peters, K.E., Walters, C., Woolhouse, A.D., Weston, R.J., Boudou, J.-P., 1998. Predicting generation and expulsion of paraffinic oil from vitrinite-rich coals. Organic Geochemistry 29, 1–21.

Koopmans, M.P., Rijptra, W.I.C., Klapwijk, M.M., de Leew, J.W., Lewan, M.D., Sinninghe Damsté, J.S., 1999. A thermal and chemical degradation approach to decipher pristane and phytane precursors in sedimentary organic matter. Organic Geochemistry 30, 1089–1104.

Levenshtein, M.L., Spirina, O.I., Nosova, K.B., Dedov, V.S., 1991. Map of Coal Metamorphism in the Donetsk Basin (Paleozoic surface), 1:500000. Ministry of Geology of the USSR, Kiev.

Lijmbach, G.W.M., 1975. On the origin of petroleum. Proc. 9th World Pet. Congr, vol. 2. Applied Science Publisher, London, pp. 357–369.

Littke, R., Horsfeld, B., Leythaeuser, D., 1989a. Hydrocarbon distribution in coals and in dispersed organic matter of different maceral compositions and maturities. Geologische Rundschau 78, 391–410.

Littke, R., Leythaeuser, D., Radke, M., Schaefer, R.G., 1989b. Petroleum generation and migration in coal seams of the Carboniferous Ruhr Basin, northwest Germany. Organic Geochemistry 16, 247–258.

Lopez-Gamundi, O.R., 1997. Glacial-postglacial transition in the late Paleozoic basins of southern south America. In: Martini, I.P. (Ed.), Late Glacial and Postglacial Environmental Changes, Quaternary, Carboniferous–Permian and Proterozoic. Oxford University Press, pp. 147–168.

Lutugin, L.I, Stepanov, P.I., 1913. Donets Coal Basin. Review of Coal Deposits of Russia.

Maystrenko, Y., Stovba, S., Stephenson, R., Bayer, U., Menyoli, E., Gajewski, D., Huebscher, C., Rabbel, W., Saintot, A., Starostenko, V., Thybo, H., Tolkunov, A., 2003. Crustal-scale pop-up structure in cratonic lithosphere: DOBRE deep seismic reflection study of the Donbas fold belt, Ukraine. Geology 31, 733–736.

Menning, M., Weyer, D., Drodzewski, G., Van Ameron, H.W.J., 1997. Carboniferous time scales 1997, time scale A (min. ages) and time scale B (max. ages). Use of geological time indicators. Carboniferous Newsletter 15, 26–31.

Miller, K.B., West, R.R., 1993. A reevaluation of Wolfcampian cyclothems in eastern Kansas: significance of subaerial exposure and flooding surfaces. Current Research in Kansas Geology. Kansas Geological Survey Bulletin 235, 1–26.

Miller, K.B., McMahon, T.J., West, R.R., 1996. Lower Permian (Wolfcampian) paleosol-bearing cycles of the U.S. midcontinent: evidence of climatic cyclicity. Journal of Sedimentary Research 66, 71–84.

Moldovan, J.M., Albrecht, P., Philp, R.P., 1992. Biological Markers in Sediments and Petroleum. Prentice Hall, New York. 411 pp.

Noble, R.A., Alexander, R., Kagi, R.I., Knox, J., 1985a. Identification of some diterpenoid hydrocarbons in petroleum. Advances in Organic Geochemistry 10, 825–829.

Noble, R.A, Alexander, R., Kagi, R.I., Knox, J., 1985b. Tetracyclic diterpenoid hydrocarbons in some Australian coals, sediments and crude oils. Geochimica et Cosmochimica Acta 49, 2141–2147.

Olszewski, T.D., Patzkowsky, M.E., 2003. From cyclothems to sequences: the record of eustasy and climate on an icehouse epeiric platform (Pennsylvanian–Permian, North American midcontinent). Journal of Sedimentary Research 73, 15–30.

Ourisson, G., Albrecht, P., Maxwell, J.R., Wheatley, R.E., 1979. The hopanoids, Palaeochemistry and biochemistry of a group of natural products. Pure and Applied Chemistry 51, 709–729.

Pepper, A.S., Corvi, P.J., 1995. Simple kinetic models of petroleum formation: Part I. Oil and gas generation from kerogen. Marine and Petroleum Geology 12, 291–319.

Perlmutter, M.A., Matthews, M.D., 1989. Global cyclostratigraphy—a model. In: Cross, T.A. (Ed.), Quantitative Dynamic Stratigraphy. Prentice Hall, New Jersey, pp. 233–260.

Peters, K.E., 1986. Guidelines for evaluating petroleum source rock using programmed pyrolysis. American Association of Petroleum Geologists Bulletin 70, 318–329.

Peters, K.E., Moldowan, J.M., 1993. The Biomarker Guide. Interpreting Molecular Fossils in Petroleum and Ancient Sediments. Prentice Hall, New Jersey. 363 pp.

Phillips, T.L., Peppers, R.A., 1984. Changing patterns of Pennsylvanian coal-swamp vegetation and implication of climatic control on coal occurrence. International Journal of Coal Geology 3, 205–251.

Philp, R.P., 1985. Fossil fuel biomarkers. Methods in Geochemistry and Geophysics. Elsevier, New York, p. 294.

Philp, R.P., 1994. Geochemical characteristics of oils derived predominantly from terrigenous source materials. In: Scott, A.C., Fleet, A.J. (Eds.), Coal and Coal-Bearing Strata as Oil-Prone Source Rocks. The Geological Society, London, pp. 71–91.

Philp, R.P., Mansuy, L., 1997. Petroleum geochemistry: concepts, applications, and results. Energy Fuels 11, 749–760.

Piedad-Sánchez, N., Suárez-Ruiz, I., Martinez, L., Izart, A., Elie, M., Keravis, D., 2004. Organic petrology and geochemistry of the Carboniferous coal seams from the Central Asturian Coal Basin (NW Spain). International Journal of Coal Geology 57, 211–242.

Piedad-Sánchez, N.I., Martinez, L., Izart, A., Suárez-Ruiz, I., Elie, M., Menetrier, C., 2005. Artificial maturation of a high volatile bituminous coal from Asturias (NW Spain) in a confined pyrolysis system: Part I. Petrographic, geochemical and molecular studies. Journal of Analytical and Applied Pyrolysis 74, 61–76.

Popov, V.S., 1963. Tectonics of the Donets Basin (in Russian). In: Kuznetzov, I.A. (Ed.), Geology of Coal and Oil Shale Deposits of the USSSR, vol. 1. Nedra, Moscow, pp. 103–151.

Privalov, V.A., Panova, E.A., Azarov, N.Ya., 1998. Tectonic events in the Donets Basin: spatial, temporal and dynamic aspects (in Russian). Geologiya i Geohimiya Goruchykh Kopalin (Geology and Geochemistry Fossil Fuels) 4, 11–18.

Privalov, V.A., Izart, A., Sachsenhofer, R.F., Antsiferov, V.A., 2003. Biomarkers in coal and the study of the formation of hydrocarbons in the Donets Basin (in Russian). Naukovy Visnyk of National Mining University (Dnjepropetrovsk) 6, 42–46.

Privalov, V.A., Izart, A., Sachsenhofer, R.F., Zhykalyak, M.V., Panova, E.A., 2003. Oil and gas generation potential of Donbas coals: results of thermolytic gas chromatography (in Russian). Ukrainian Geologist (Kiev) 3-4, 56–59.

Radke, M., Welte, D.H., 1983. The methylphenanthrene index (MPI): a maturity parameter based on aromatic hydrocarbons. In: Bjoroy, M., et al., (Eds.), Advances in Organic Geochemistry. J. Wiley and sons, New York, pp. 504–512.

Radke, M., Schaefer, R.G., Leythaeuser, D., 1980. Composition of soluble organic matter in coals: relation to rank and liptinite fluorescence. Geochimica et Cosmochimica Acta 44, 1787–1800.

Rohmer, M., Bisseret, P., Neunlist, S., 1992. The hopanoids, prokaryotic triterpenoids and precursors of ubiquitous molecular fossils. In: Moldowan, J.M., Albrecht, P., Philp, R.P. (Eds.), Biological Markers in Sediments and Petroleum. Prentice Hall, New York, pp. 1–17.

Sachsenhofer, R.F., Privalov, V.A., Zhykalyak, M.V., Bueker, C., Panova, E., Rainer, T., Shymanovskyy, V.A., Stephenson, R., 2002. The Donets Basin (Ukraine/Russia): Coalification and thermal history. International Journal of Coal Geology 49, 33–55.

Sachsenhofer, R.F., Privalov, V.A., Izart, A., Elie, M., Kortensky, J., Panova, E.A., Sotirov, A., Zhykaliak, M.V., 2003. Petrography and geochemistry of Carboniferous coal seams in the Donets Basin (Ukraine): implications for palaeoecology. International Journal of Coal Geology 55, 225–259.

Stephenson, R.A., Stovba, S.M., Starostenko, V.I., 2001. Pripyat–Dniepr–Donets Basin: implications for dynamics of rifting and the tectonic history of the northern Peri–Tethyan platform. In: Ziegler, P.A., et al., (Eds.), Peri–Tethyan Rift/Wrench Basins and Passive Margins, Peri–Tethys Memoir 6, vol. 186. Mémoires du Muséum National d́Histoire Naturelle, Paris, pp. 369–406.

Sterlin, B.P., Makridin, V.P., Lutsky, P.I., 1963. Stratigraphy of Mesozoic and Cenozoic deposits of the Donets Basin (in Russian). Geology of Coal and Oil Shale Deposits of the USSR, vol. 1. Nedra, Moscow, pp. 64–88.

Stovba, S.M., Stephenson, R.A., 1999. The Donbas Foldbelt: its relationships with the uninverted Donets segment of the Dniepr–Donets Basin, Ukraine. Tectonophysics 313, 59–83.

Strehlau, K., 1990. Facies and genesis of Carboniferous coal seams of Northwest Germany. International Journal of Coal Geology 15, 245–292.

Sykes, R., Snowdon, L.R., 2002. Guidelines for assessing the petroleum potential of coaly source rocks using Rock–Eval pyrolysis. Organic Geochemistry 33, 1441–1455.

Taylor, G.H., Teichmüller, M., Davis, A., Diessel, C.F.K., Littke, R., Robert, P., 1998. Organic Petrology. Gebrüder Borntraeger, Berlin. 704 pp.

ten Haven, H.L., de Leeuw, J.W., Rullkötter, J., Sinninghe Damste, J.S., 1987. Restricted utility of the pristane/phytane ratio as a palaeoenvironmental indicator. Nature 330, 641–643.

Tissot, B.P., Welte, D.H., 1984. Petroleum Formation and Occurrence, 2nd ed. Springer-Verlag, Berlin. 699 pp.

Van der Zwan, C.J., 1981. Palynology, phytogeography and climate of the lower Carboniferous. Paleogeography, Paleoclimatology, Paleoecology 33, 279–310.

Van der Zwan, C.J., Boulter, M.C., Hubbard, R.N.L.B., 1985. Climatic change during the lower Carboniferous in Euramerica, based on multivariate statistical analysis of palynological data. Paleogeography, Paleoclimatology, Paleoecology 52, 1–20.

Van Wagoner, J.C., Posamentier, H.W., Mitchum, R.M., Vail, P.R., Sarg, J.F., Loutit, T.S., Hardenbol, J., 1988. An overview of the fundamentals of sequence stratigraphy and key definitions. In: Wilgus, C.K., Hastings, B.S., Ross, A., Posamentier, H., Van Wagoner, J., Kendall, C.G.St.C. (Eds.), Sea-level Changes: An Integrated Approach, Soc. Economic Paleontologists and Mineralogists,Sp. Pub., vol. 42, pp. 39–45.

Vliex, M., Hagemann, H.W., Püttmann, W., 1994. Aromatized arborane/fernane hydrocarbons as molecular indicators of floral changes in Upper Carboniferous/Lower Permian strata of the Saar–Nahe Basin, southwestern Germany. Geochimica et Cosmochimica Acta 58, 4689–4702.

Volkman, J.K., 1986. A review of sterol markers for marine and terrigenous organic matter. Organic Geochemistry 9, 83–99.

Volkman, J.K., 2005. Sterols and other triterpenoids: source specifity and evolution of biosynthetic pathways. Organic Geochemistry 36, 139–159.

Volkman, J.K., Maxwell, J.R., 1986. Acyclic isoprenoids as biological markers. In: Johns, R.B. (Ed.), Biological Markers in the Sedimentary Record. Elsevier, pp. 1–42.

Volkman, J.K., Barrett, S.M., Blackburn, S.I., Mansour, M.P., Sikes, E.L., Gelin, F., 1998. Microalgal biomarkers: a review of recent research developments. Organic Geochemistry 29, 1163–1179.

Volkman, J.K., Barrett, S.M., Blackburn, S.I., 1999. Eustigmatophyte microalgae are potential sources of C_{29} sterols, C_{22}–C_{28} *n*-alcohols and C_{28}–C_{32} *n*-alkyl diols in freshwater environments. Organic Geochemistry 30, 307–318.

Ziegler, A.M., Hulver, M.L., Rowley, D.B., 1997. Permian world topography and climate. In: Martini, I.P. (Ed.), Late Glacial and Postglacial Environmental Changes, Quaternary, Carboniferous–Permian and Proterozoic. Oxford University Press, pp. 111–146.